THE ASTROPHYSICAL JOURNAL, 277:333–354, 1984 February 1

ON THE FREQUENCY OF PLANETARY NEBULA NUCLEI POWERED BY HELIUM BURNING AND ON THE FREQUENCY OF WHITE DWARFS WITH HYDROGEN-DEFICIENT ATMOSPHERES[1]

ICKO IBEN, JR.
University of Illinois
Received 1983 March 30; accepted 1983 July 19

ABSTRACT

The evolutionary behavior of a model central star of a planetary nebula is examined as a function of the phase in its nuclear burning cycle when its progenitor leaves the asymptotic giant branch for the first time. Models may be assigned to one of six distinct groups, and estimates may be made of the probability that a real star will fall into a particular group. In particular, it is suggested that approximately 25% of all central stars of planetary nebulae will fall into groups whose members are expected to become hydrogen-deficient white dwarfs. This suggestion is not in disagreement with the observations. It is argued that winds of at least two types are responsible for this result: a low-velocity or slow wind (of ordinary or super strength) which operates when, and if, the central star returns to the asymptotic giant branch after experiencing a final helium shell flash; and a high-velocity or fast wind which operates when the central star is at high enough surface temperatures that emitted photons will excite nebular emission. It is also inferred that roughly half of all bright central stars of planetary nebulae are burning helium rather than hydrogen. Finally, an attempt is made to assess the relevance of extant models for understanding exotic planetary nebulae such as A30 and A78, helium-rich stars of the R Coronae Borealis variety, and the chameleon star FG Sagittae.

Subject headings: nebulae: planetary — stars: evolution — stars: interiors — stars: stellar statistics — stars: white dwarfs

I. PREAMBLE—AGB STARS, WINDS, PLANETARY NEBULAE, AND WHITE DWARFS

In recent years it has become clear that stellar winds of perhaps several distinct types play an important role in mediating the transformation of asymptotic giant branch (AGB) stars into hot, compact objects, some of which may be the central stars of planetary nebulae. Planetary nebulae themselves are thought to be composed of matter ejected by low-velocity winds which operate either during the extended AGB phase or/and at the termination of the AGB phase. During the hot, compact phase of evolution, additional high-velocity winds may impact the nebular material formed by the prior low-velocity winds and influence its structure. Unfortunately, the nature and strength of these winds cannot as yet be estimated from first principles, and our entire knowledge of their importance rests on observational evidence.

While on the AGB, all single stars of initial main-sequence mass less than about 9 $M_\odot$ are thought to lose mass more or less continuously via what we shall here call an "ordinary wind." This ordinary wind is often parameterized by the expression (Reimers 1975*a*, *b*)

$$\dot{M}_{\rm OW} = -4 \times 10^{-13} \eta (LR/M)\, M_\odot \ {\rm yr}^{-1}\,, \qquad (1)$$

where L = stellar luminosity, R = stellar radius, M = stellar mass, all in solar units, and η is an adjustable parameter determined semiempirically to be in the range $\frac{1}{3}$–3.

From the fact that, in Galactic globular clusters, the tip of the AGB is approximately as luminous as the tip of the first red giant branch, it may be estimated (Fusi-Pecci and Renzini 1976; Renzini 1981*b*) that, at least for luminosities on the order of or less than $L \sim 3 \times 10^3\ L_\odot$, $\eta \sim 0.4$. Similarly, from a consideration of how the extent of the AGB in intermediate age clusters in the Magellanic Clouds depends on estimated cluster age, one may guess that a value of $\eta \sim \frac{1}{3}$–$\frac{1}{2}$ is also appropriate for luminosities as large as $L \sim 10^4$ (e.g., Iben and Renzini 1983). Further, Wood and Cahn (1977) find a value of $\eta \sim \frac{1}{3}$ to be appropriate for Mira variables in the Galaxy.

It is relevant to compare the mass loss rate of the ordinary wind with the rate at which nuclear processes affect the evolution of stellar characteristics. During the thermally pulsing portion of the AGB phase (the TP-AGB phase), hydrogen and helium burn alternately in two shells, with periods of quiescent burning separated by a helium shell flash. The duration of the quiescent helium-burning phase is roughly 10% of the quiescent hydrogen-burning phase, this fraction being a consequence of the facts that (1) the exploitable nuclear energy content of 1 g of helium is approximately 1/10 that of 1 g of hydrogen, and (2) the mean luminosities during the two burning phases are roughly the same. A measure of the mean luminosity during quiescent hydrogen burning is the expression

$$L \sim 6 \times 10^4 (M_{\rm H} - 0.5)\,, \qquad (2)$$

where $M_{\rm H}$ is the location of the center of the hydrogen profile, and both L and $M_{\rm H}$ are in solar units. During the quiescent hydrogen-burning phase, the hydrogen-burning shell advances at the rate

$$\dot{M}_{\rm H} \sim 6 \times 10^{-7} X_{\rm H}^{-1} (M_{\rm H} - 0.5)\, M_\odot \ {\rm yr}^{-1}\,, \qquad (3)$$

[1] Supported in part by the NSF grant AST 81-15325.

where X_H is the surface abundance by mass of hydrogen. A final ingredient necessary for a comparison between $\dot{M}_H$ and $\dot{M}_{OW}$ is the dependence of stellar radius on L and M. In fair approximation (Iben 1983)

$$R \approx 312(L/10^4)^{0.68}(1.175/M)^{0.31S}(Z/0.001)^{0.088}/(l/H)^{0.52}\,, \tag{4}$$

where Z = abundance by mass of heavy elements, l/H = mixing length to pressure scale height, and $S = 0$ for $M \lesssim 1.175$ and $S = 1$ otherwise. This expression is valid as long as the mass in the hydrogen-rich envelope is not small compared with the mass in the helium-rich zone below it.

Combining equations (1)–(4) and choosing as an example $X_H = 0.75$, $Z = 0.001$, $l/H = 1$, and $M < 1.175$, one has

$$\dot{M}_{OW}/\dot{M}_H \sim -0.03\eta R/M \sim -2.6\eta(L/10^3)^{0.68}/M \sim -(32\eta/M)(M_H - 0.5)^{0.68}\,. \tag{5}$$

For the large majority of appropriate choices of M and M_H, including those focussed upon in later sections ($M_H \sim 0.6$ and $M < 1$, $\dot{M}_{OW}/\dot{M}_H \sim -6.1\eta/M$), it is evident that the mass M_e in the hydrogen-rich envelope ($M_e = M - M_H$) decreases more rapidly due to wind mass loss than due to nuclear burning.

Once M_e drops below $M_{eD} \sim 0.2\Delta M_H$, where ΔM_H is the mass through which the hydrogen-burning shell advances between thermal pulses, equation (4) is no longer valid and R becomes an extremely sensitive function of M_e, decreasing rapidly with decreasing M_e. If the AGB star is in a hydrogen-burning phase and M_e falls below M_{eD}, the star departs from the AGB and the ordinary wind (if still governed by eq. [1]) becomes rapidly less important than nuclear burning in reducing M_e. The nature of evolution as (and if) it is controled by $\dot{M}_H$ and $\dot{M}_{OW}$ was first extensively explored by Schönberner (1979), who showed that a final helium shell flash may occur as the star makes the transition at high luminosity to the hot, compact state or even, in a few instances, after it has ceased hydrogen burning and has begun the descent of the white dwarf cooling sequence.

Whether or not this sort of conjectural evolution will produce an observable planetary nebula (PN, plural PNe) depends upon whether or not the post-AGB star emits a "hot" wind of sufficient strength and duration to compress the material ejected during the prior AGB phase to large enough densities (Kwok, Purton, and Fitzgerald 1978; Kwok 1982, 1983). That is, one requires that the total momentum delivered by the hot wind $|\dot{M}_{HW} V_{HW} \Delta t_{HW}|$ be much greater than $M_{PN} V_{PN}$. Here $\dot{M}_{HW}$, V_{HW}, and Δt_{HW} are, respectively, the mass loss rate, the mean velocity, and the duration of the hot wind, and M_{PN} and V_{PN} are, respectively, the mass and the velocity of the resultant condensed nebula.

Analysis of *IUE* observations (Heap 1979, 1980, 1983; Perinotto, Benvenuti, and Cacciari 1981; Castor, Lutz, and Seaton 1981; Perinotto 1983) show that hot central stars of several PNe produce winds at rates $\dot{M}_{HW} \sim -(5\text{–}200) \times 10^{-9}$ $M_\odot$ yr^{-1} and at velocities $V_{HW} \sim (1000\text{–}3000)$ km s^{-1}. The momentum transferred by hot winds with velocities near the middle of the observed range would appear to be too small by perhaps an order of magnitude to produce a "typical" PN of mass $M_{PN} \sim 0.2\ M_\odot$, expansion velocity $V_{PN} \sim 20$ km s^{-1}, and age $\sim 10^4$ yr. Another problem with this picture is that the size of the region filled with material emitted by the ordinary wind is quite large compared with the radii of typical PNe, so that only a fraction of the emitted material may be called upon (perhaps not enough) to explain the typical PN. Nevertheless, there are extremely large uncertainties in estimates of all relevant quantities (in particular, of $\dot{M}_{HW}$ and of M_{PN}), and it is entirely possible that some observed PNe are the result of the compression by a hot wind from a central star of circumstellar matter which has been produced by an "ordinary" wind which operates during an earlier AGB phase of evolution.

One interpretation of the characteristics of typical PNe and of their associated central stars or nuclei (PNNi, singular PNN) is that PN and PNN formation occurs as a coordinated event over a time τ_{ej} which is short compared with the expansion age τ_{ex} of the PN (Shklovski 1956) and that the "transition" time τ_{tr} for the central star to achieve a surface temperature high enough to produce ionizing photons ($T_e > 30{,}000$ K) must also be short compared with τ_{ex} (Härm and Schwarzschild 1975; Renzini 1979, 1981*b*). The requirement $\tau_{ej} < \tau_{ex}$ implies an effective mass loss rate during the main "ejection" event which removes mass from the star at least as rapidly as $\dot{M} = -M_{PN}/\tau_{ex}$ ($\sim -10^{-5}\ M_\odot$ yr^{-1} for $M_{PN} \sim 0.2\ M_\odot$ and $\tau_{ex} \sim 2 \times 10^4$ yr). In general, estimates of $|\dot{M}_{ej}|$ are at least an order of magnitude larger than $|\dot{M}_{OW}|$ with $\eta \gtrsim 1$, and it is convenient (and colorful) to call the associated mass loss process a "superwind" (Renzini 1981*a*). It is implicitly assumed that the mechanism which drives a superwind is different from that which drives the ordinary wind.

If the superwind is initiated during the hydrogen-burning phase, the mass M_{eR} remaining in the hydrogen-rich envelope after the ejection event must be on the order of or less than $M_{eD} \sim 0.2\Delta M_H$; for values of $M_e > M_{eD}$ the central star remains on the AGB with a structure which can presumably continue to support rapid mass ejection. If ejection occurs during the high-luminosity phase following a helium shell flash, the value of M_e which is small enough to allow the PNN to depart from the AGB on a rapid time scale (and thus presumably lead to termination of the superwind phase) is much smaller than M_{eD}. Finally, if ejection occurs during the subsequent quiescent helium burning phase, departure from the AGB occurs for values of M_e somewhat larger than M_{eD}. These results will be demonstrated in later sections.

The requirement that $\tau_{tr} < \tau_{ex}$ places additional constraints on M_{eR} for those stars which produce observable PNe. For example, for those stars that depart from the AGB while burning hydrogen, one may write

$$\tau_{tr} = (M_{eR} - M_{eN})/\dot{M}_H \sim \tau_{ip}(M_{eR} - M_{eN})/\Delta M_H\,, \tag{6}$$

where τ_{ip} is the time interval between thermal pulses of the precursor AGB star, and M_{eN} is the envelope mass when the PNN achieves a surface temperature large enough to excite the PN. In deriving equation (6), advantage has been taken of the fact that $\dot{M}_H$ is essentially the same for the PNN as for its AGB precursor. In first approximation, $M_{eN} \sim 0.1\Delta M_H$ (Iben 1982), and the requirement that $\tau_{tr} < \tau_{ex}$ can be met by choosing a suitably small value of M_{eR} or by choosing a suitably large value of M_H (τ_{ip} decreases quite rapidly with increasing M_H). If ejection occurs during the helium-burning

phase, the situation is more complicated, as will be described in later sections. Exploration of the evolution of model PNNi that are formed in a superwind event which occurs during the hydrogen-burning phase on the AGB was pioneered by Paczyński (1970). Evolution of PNNi following a superwind phase which occurs just after a helium shell flash was first studied by Härm and Schwarzschild (1975), but see also Rose and Smith (1969).

The occurrence of superwinds appears to be observationally well established. There is direct evidence that such winds are emitted by very bright Galactic carbon stars (Knapp *et al.* 1982) and by luminous Galactic OH/IR sources (Werner *et al.* 1980; Baud *et al.* 1981; Baud and Habing 1983), and there is evidence that the strength of these winds increases with stellar luminosity and, in general, with increasing initial main sequence mass (de Jong 1983). Indirect evidence also exists in the form of AGB number-luminosity distributions for field stars and for intermediate-age globular clusters in the Magellanic Clouds. When compared with theoretical predictions based on the assumed operation of an ordinary wind, the scarcity of AGB stars at magnitudes brighter than $M_{\rm BOL} \sim -6$ in the Cloud globular clusters (Frogel 1983) and the infrequency in the Clouds of long period variables which are also AGB stars (Wood, Bessell, and Fox 1983), suggest mass loss rates for bright AGB stars which are at least an order of magnitude more effective than $\dot{M}_{\rm OW}$ with $\eta \sim \frac{1}{3}$ (Frogel and Iben 1983). Of course, whether this means that a superwind sets in when stellar luminosity exceeds a critical value or simply that the ordinary wind is relatively more robust at high luminosity (with η being an order of magnitude larger for bright AGB stars than it is for dim ones) is, at this stage, to some extent a matter of semantics.

It must not be forgotten that there is good evidence for the operation of an ordinary wind ($\eta < 1$) during a substantial fraction of an AGB star's lifetime. For example, it would be impossible to account for the observed number and distribution in luminosity of AGB stars in the Magellanic Clouds if typical TP-AGB lifetimes for stars with luminosities dimmer than $M_{\rm BOL} \sim -6$ were much less than $\sim 10^6$ yr. In fact, taking into account mass loss during the pre–thermally pulsing AGB phase, it is possible to show that even an ordinary wind as approximated by equation (1) with $\eta = 1$ will cause all AGB stars of initial mass less than $\sim 2\ M_\odot$ to evaporate their hydrogen-rich envelopes before they reach the thermally pulsing stage (Frogel and Iben 1983). The development of a surface carbon abundance greater than the surface oxygen abundance requires a sequence of events that occurs only in TP-AGB stars, and, therefore, the existence of copious numbers of carbon stars in the Clouds with $M_{\rm BOL}$ in the range $-4 > M_{\rm BOL} > -6$ rules this possibility out quite emphatically.

The picture one forms, then, is that, during the first portion or every star's AGB lifetime, a mild wind operates, but if and when the star's structure achieves some critical configuration, a superwind sets in. It is as yet uncertain as to what constitutes a critical configuration, but several theoretical studies suggest that the superwind mass loss is brought about by an unbridled growth in pulsation amplitude when the star becomes unstable to acoustical pulsation in the fundamental radial mode (Wood 1974, 1981). There are enough uncertainties in the calculations and an insufficient exploration of parameter space has been made to form a clear idea as to what exactly the crucial determining factors are, but it appears that the instability sets in when L exceeds a critical value which presumably depends on M and also on M_e (Wood 1974, 1981; Tuchman, Sack, and Barkat 1979; Willson 1981; Fadeyev 1982).

In summary, the observations suggest that winds of at least three different types (and presumably of three different origins) play a role in the life of a star as it makes its way from the AGB, through a hot, compact phase at high luminosity, to the cooling white dwarf state. Further, there may be at least two different ways of producing PNe: by mass ejection at a high rate and by mass ejection at a smaller rate followed by hot wind compression. The indication that a critical luminosity must be exceeded in order for a superwind to be triggered (see also Weidemann 1975) suggests that the probability for superwind PN formation increases with increasing initial stellar mass. The fact that perhaps 30% or more of all known PNe exhibit double shells (Kaler 1974) suggests that, in some instances, both formation mechanisms may operate: a hot wind compressing the matter at the inner edge of a PN which was initially produced by a superwind might lead to the appearance of a double shell. Finally, it must be emphasized that, although all AGB stars produce circumstellar shells, it may be that not all, if indeed most, post-AGB stars produce observable PNe.

Just as the analysis of PN characteristics may provide some clue as to the nature of the winds that produce them, analysis of the surface composition of white dwarfs may provide clues as to the nature and strength of these same winds and clues as to the phase in the nuclear-burning life of the precursor star at which this precursor star departed from the AGB. For the purposes of this paper, what one would most like to know is the fraction of white dwarfs which do not exhibit hydrogen at their surfaces. Since gravitational settling is very effective in reducing surface composition to the lowest molecular weight possible (Schatzman 1958), and since convective mixing does not operate to reduce an initial surface hydrogen abundance until surface temperatures fall below $\sim 13{,}000$ K (D'Antona and Mazzitelli 1975; Fontaine and Van Horn 1976; Koester 1976; Vauclair and Reisse 1977; D'Antona and Mazzitelli 1979), hot white dwarfs which are hydrogen deficient (non-DA) must have as precursors stars which have lost their entire hydrogen-rich envelopes via winds.

Among all white dwarfs hotter than 45,000 K in the Palomar Green Survey of blue stellar objects, approximately 15% are non-DA; out of the total sample of 359 white dwarfs hotter than 12,000 K, approximately 12% are non-DA (Green and Liebert 1983; see also Oke *et al.* 1984). Out of the roughly 750 white dwarfs which have been spectroscopically classified prior to 1979, approximately one-third are of the non-DA variety (Sion 1979; see also Sion and Liebert 1977; Liebert 1979, 1980). The mean surface temperature of stars in the Sion sample is thought to be less than that of stars in the Green sample and this may indicate that there is a tendency for the non-DA/DA ratio to increase with decreasing T_e (Green and Liebert 1983). This is in accord with the classification scheme of D'Antona and Mazzitelli (1979) which suggests that the frequency of DA (hydrogen-rich), DB (helium-rich), and DC (helium-rich) white dwarfs is, respectively, highest at large T_e, intermediate T_e, and low T_e. Since white dwarfs dim as they cool, the statistics also mean that the fraction of non-DA white dwarfs

increases with decreasing luminosity, a fact that is shown directly by Sion (1979).

A primary objective of this paper is to suggest that the precursors of non-DA white dwarfs are stars which have experienced a helium shell flash either during a post-AGB phase or just prior to departing from the AGB for the first time. One implication of these estimates is that a significant fraction of the brightest PNNi may be burning helium rather than hydrogen in a shell.

The mechanism which transforms a hot, compact PNN with a hydrogen-rich surface into one with a hydrogen-deficient surface is suggested to be simply a wind which strips off successive layers of matter from the surface until, first, matter which has experienced complete hydrogen burning is exposed (these include the progenitors of DB white dwarfs) and, then, matter which has experienced partial helium burning is exposed (these may become DC white dwarfs when they have cooled to such an extent that C_2 bands can be seen). This has also been suggested by Renzini (1979). The role of a helium shell flash in an immediate precursor star is twofold. First, relative to its preflash values, the amount of matter that is in the hydrogen-rich envelope is considerably reduced by one of two processes: either this matter experiences a second phase of hydrogen burning during the flash (this is estimated to occur in roughly 10% of all cases) or the star becomes a "born-again" AGB star as a consequence of flash-engendered expansion and loses matter from the surface via a low-velocity (super)wind (this is estimated to occur in roughly 15% of all cases). Second, a high-velocity wind which operates during the postflash PNN phase (on a long quiescent helium-burning time scale) and during the initial high-luminosity portion of the white dwarf cooling phase (tapping the reservoir of thermal energy built up during the shell flash) continues to strip off matter from the surface until nearly pure helium layers are exposed and then, in some instances, carbon-rich, helium-rich layers are exposed.

In the following four sections, the manner in which a post-AGB model of low mass evolves will be explored as a function of the phase in its nuclear burning cycle at which it departs from the AGB. In these sections, no attempt will be made to assess whether departure is more likely to be due to an ordinary wind or to a superwind and the effect on evolutionary time scales of a hot wind operating during the post-AGB phases will not explicitly be taken into account in the calculations. For convenience, all models will be called PNNi, whether or not they will produce observable PNe, and the circumstellar shells around them will be called PNe, whether observable or not. Further, the terms "first departure from the AGB" and "PN ejection event" will be used interchangeably. The resultant models may be roughly categorized into four groups (a more extended classification scheme will be introduced in § VII).

Members of the first group (type I in § VII) depart from the AGB during the extended hydrogen-burning interpulse phase and continue to burn hydrogen as hot, compact objects until envelope mass drops below a critical value. At this point hydrogen burning via the CN cycle ceases and an ensuing brief phase of rapid contraction and luminosity decrease is followed by an extended cooling phase. During this latter phase, a stellar wind may continue to strip hydrogen-rich matter from the surface, but probably not at a sufficiently high rate to convert these models ultimately into non-DA white dwarfs.

Members of another class of PNN models (type II in § VII) experience a helium shell flash after hydrogen burning at high T_e has ceased (Fujimoto 1977; Schönberner 1979). During the flash most of the hydrogen remaining near the surface of each model is engulfed by the convective shell and burned. During the ensuing quiescent helium-burning phase, these models may be expected to lose mass via a fast, high-temperature wind which will rapidly expose helium- and carbon-rich layers; thus, these models are expected to develop hydrogen-deficient surfaces shortly after embarking on the extended helium-burning phase (Iben *et al.* 1983).

After departing from the AGB while burning hydrogen, members of a third class of theoretical models (types III and IV in § VII) experience a final helium shell flash which carries each model *back* to the AGB where the mechanism which produced the PNN in the first place might be expected to operate a second time. During this second ascent of the AGB, hydrogen does not burn, and the hydrogen profile, the base of which separates the underlying helium-rich region from the extended hydrogen-rich envelope, lies within the outer envelope at a much larger distance from the center and therefore at a lower potential than during the first ascent. Thus, whereas the first AGB (super?)wind phase is terminated long before the center of the hydrogen profile is exposed at the surface, the second AGB (super?)wind phase may lead to the ejection of much of the remaining hydrogen-rich matter into a secondary nebular shell of small mass ($< M_{eR}$). The remnant core will then rapidly evolve to high temperature where it excites the secondary nebular shell and possibly also reexcites the first nebular shell, provided that this shell has not expanded to such an extent that its surface brightness is below the limit of detectability. During the subsequent extended phase of quiescent helium burning, the PNN loses mass via a hot wind, possibly to such an extent that, toward the end of the burning phase or after, all vestiges of hydrogen-rich material are ultimately removed. Thus, these models, too, are expected to develop hydrogen-deficient surfaces, but at a much later stage in their evolution than do models which experience a helium shell flash after hydrogen burning has ceased.

Members of a final class of PNN models (types V and VI in § VII) depart from the AGB following a helium shell flash and burn helium quiescently at sufficiently high T_e to excite the surrounding PN. These models do not become giants again. Whether they will subsequently reignite hydrogen depends on the amount of hydrogen-rich matter they retain following the initial PN ejection event, and whether they become non-DA white dwarfs depends on whether they lose sufficient mass as PNNi. Types I, II, and IV (in the notation of § VIII) have been discussed qualitatively by Renzini (1982), and his suggestions are confirmed by the quantitative calculations reported here.

Having described the major types of theoretical PNN evolution at constant mass in §§ II–V, mass loss is introduced explicitly in § VI, and the probability of forming non-DA white dwarfs under various assumptions is discussed in § VII. Finally, in § VIII, comments on the relevance of calculated models to the planetary nebulae A30 and A78 and to the FG Sagittae and R CrB phenomena are made.

II. PNN EVOLUTION AT CONSTANT MASS—THE CASE OF PURE HYDROGEN BURNING

In this and in the following three sections, we explore the consequence of assuming that departure from the AGB following PN ejection occurs at an arbitrary point during the AGB phase. Although mass loss following this first departure is not included explicitly in the calculations, it will be made clear that such mass loss probably plays a crucial role in real PNN evolution.

In order to establish an appropriate universe of discourse, we define (in some cases for a second time) a number of relevant quantities, each having the dimension of mass:

M_e = mass in the hydrogen-rich envelope of the PNN = mass between the stellar surface and the center of the hydrogen-burning shell (or the center of the hydrogen profile, if hydrogen is not burning) = $M - M_H$.

M_{eD} = envelope mass when stellar radius R becomes very sensitive to M_e during the hydrogen-burning phase.

M_{eR} = PNN envelope mass immediately after the PN ejection event.

M_{eN} = envelope mass when the surface temperature of the PNN first exceeds 30,000 K.

M_{eI} = envelope mass when a final helium shell flash occurs and/or when hydrogen burning ceases.

M_{eF} = envelope mass when all nuclear burning has ceased.

ΔM_H = mass which the hydrogen-burning shell would process between helium shell flashes if the parent star were to remain on the AGB.

δM_H = mass actually processed by the hydrogen-burning shell following the occurrence of the last flash while the parent star is on the AGB.

$\delta M_{HD} = \delta M_H$ when stellar radius R becomes very sensitive to M_e during the hydrogen-burning phase.

$\delta M_{HR} = \delta M_H$ when the PN ejection event takes place.

$\delta M_{HN} = \delta M_H$ when T_e of the PNN first exceeds 30,000 K.

$\delta M_{HI} = \delta M_H$ when the last helium shell flash begins.

The starting model for the series of experiments to be described here is an 0.6 $M_\odot$ model which experienced its last helium shell flash while on the AGB when $M_H \approx 0.5901$ $M_\odot$. The surface abundances by mass of hydrogen, helium, and heavy elements are, respectively, $X = 0.75$, $Y = 0.25$, $Z = 0.001$; and $\Delta M_H \sim 0.01$ $M_\odot$. The prior evolution of the initial model is described elsewhere (Iben 1982). The choice of $M_H \sim 0.6$ is influenced by the Koester *et al.* (1979) demonstration that the peak in the white dwarf number versus mass distribution occurs at ~ 0.6 $M_\odot$. The choice of $Z = 0.001$ is arbitrary, and, in any case, the major inferences to be drawn from the detailed models are not expected to be particularly sensitive to the specific choice of Z.

The real analog of the starting model is presumably a star with an initial main-sequence mass considerably larger than 0.6 $M_\odot$. For example, assuming that the Reimers mass loss rate with $\eta = \frac{1}{3}$ operates during all preceding evolutionary phases, the initial mass of the real analog may be estimated to be greater than $M_{min} \sim 1.05$ $M_\odot$ and the duration of the preceding main-sequence and core helium-burning phases may be estimated to be less than 7.2×10^9 yr (Iben 1983). A total of at least 0.28 $M_\odot$ is lost during the first red giant (RG) phase and during the early AGB (E-AGB) phase prior to the thermally pulsing AGB (TP-AGB) phase. If we assume that a final superwind episode produces a PN of mass $M_{PN} = 0.2$ $M_\odot$, then the initial mass is $M_{start} \sim 1.24$ $M_\odot$, the preceding evolution has required $\sim 4.4 \times 10^9$ yr, and again approximately 0.28 $M_\odot$ has been lost during the first RG and E-AGB phases via an ordinary wind. The choice of PNN mass $M_{PNN} = 0.6$ $M_\odot$ might be considered appropriate because the number-mass distribution of white dwarfs exhibits a peak at about 0.6 $M_\odot$ (see, e.g., Koester, Schulz, and Weidemann 1979). The mass of a typical main-sequence progenitor might therefore be expected to be on the order of 1.05–1.24 $M_\odot$.

In each of the following experiments, we vary the mass of the initial model by discrete amounts (by adopting a large mass loss or mass accretion rate for a short time) and pursue the evolution of the resultant model (at constant mass $M = M_{PNN}$) through all subsequent phases until it has ceased burning nuclear fuel at a structurally significant rate. The addition of mass to achieve a given initial model has been done for convenience; one could equally well have begun with a large enough model mass on the AGB and abstracted mass, as was done to produce the initial models described in Figure 1. However, since such a procedure would give the same result and yet be more expensive, the more convenient method has been chosen.

The thick dashed curve in Figure 1 shows the evolutionary track in the H-R diagram followed by a model of mass $M_{PNN} = 0.5990$ $M_\odot$ after its envelope mass has decreased to $M_e \sim 0.0015$ $M_\odot$. The time at which the model passes each tick mark along the track is given in years and the mass in the hydrogen-rich envelope is given (in several instances) in parentheses beside that tick mark. The zero point for time is chosen as the moment when the model star achieves 30,000 K for the first time. Thus, $M_{eN} = 0.00118$ $M_\odot$. Essentially identical tracks obtain for all other hydrogen-burning models with total mass in the range 0.5913 $M_\odot \leq M_{PNN} \leq 0.599$ $M_\odot$. The only differences are that, for smaller M_{PNN}, the "plateau" luminosity, the maximum value of T_e, and the rate of evolution along a track are slightly smaller. As M_{PNN} is decreased to below 0.5904 $M_\odot$, hydrogen burning can no longer be sustained and the model must evolve to the white dwarf configuration on a thermal time scale. When M_{PNN} is in the range 0.5904 $M_\odot < M_{PNN} < 0.5913$ $M_\odot$, evolution times decrease rapidly with decreasing mass.

Along the upper or plateau portion of the track in Figure 1, the location in T_e of the hydrogen-burning model is in one-to-one correspondence with M_e, and the indicated time of evolution between successive values of T_e is a consequence of the reduction in M_e at a rate determined solely by the burning of hydrogen with M_{PNN} = constant. If one admits that the real analog of the model PNN experiences mass loss, then M_e should in reality decrease more rapidly than has been calculated, and the rate of evolution along the track should be increased. The question is, by how much? In the present instance, the rate at which M_e decreases due solely to nuclear burning is

$$\dot{M}_e \equiv \dot{M}_{e,nuc} \sim -7 \times 10^{-8}\ M_\odot\ \mathrm{yr}^{-1}\ . \qquad (7)$$

The mass loss rate derived from equation (1) (which is, in any case, quite probably not applicable) decreases in absolute

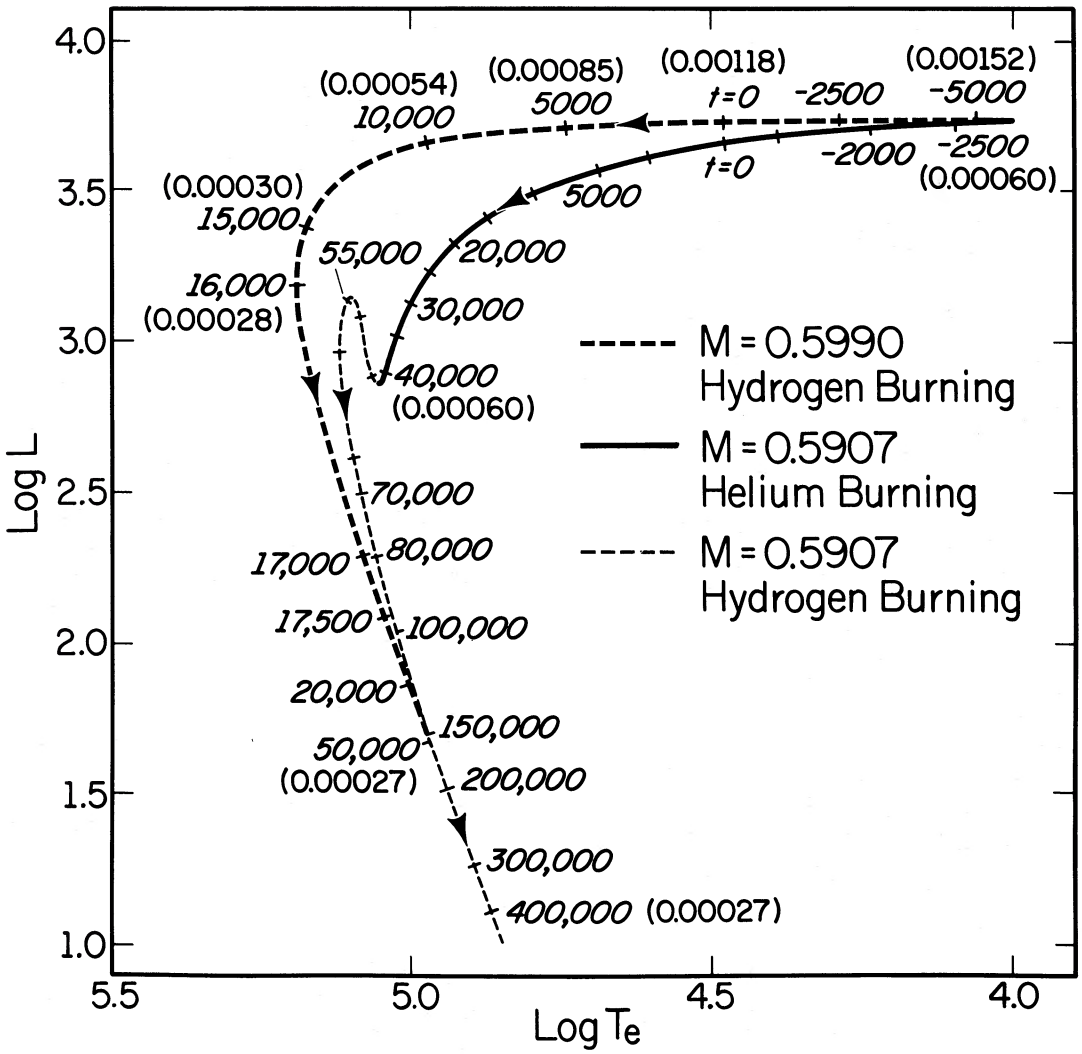

FIG. 1.—Model PNN tracks. The thick dashed track is for a model which departs from the AGB during the hydrogen-burning phase with mass $M = 0.5990\ M_\odot$. The time to reach each tick mark is given in years, and the mass M_e in the hydrogen-rich envelope is given (in parentheses) in solar units. The solid track, continuing as a thin dashed track, is for a model which departs from the AGB during the high luminosity phase which follows a helium shell flash. Its mass is $M = 0.5907\ M_\odot$ and $M_e = 0.00060\ M_\odot$ during the helium burning portion of its evolution (*solid track*). M_e decreases to its final value of $0.00027\ M_\odot$ during the first portion of the dashed track ($t \sim 40{,}000$–$65{,}000$ yr).

magnitude from $\sim 2 \times 10^{-8}\ M_\odot\ \mathrm{yr}^{-1}$ at $\log T_e = 4.0$ to $\sim 2 \times 10^{-9}\ M_\odot\ \mathrm{yr}^{-1}$ at $\log T_e = 4.5$. In obtaining these rates, η has been set equal to $\frac{1}{3}$. The mass loss rate of the wind from a PNN of luminosity similar to the plateau luminosity in Figure 1 is estimated to be $\sim 10^{-8}\ M_\odot\ \mathrm{yr}^{-1}$ (Perinotto, Benvenuti, and Cacciari 1981). It therefore appears that, as far as evolutionary changes in the H-R diagram are concerned, the assumption of constant stellar mass is perhaps a reasonable, though by no means completely satisfactory, first approximation.

We have argued that, as a consequence of a stronger (super?)wind, the rate at which M_e decreases during the preceding AGB phase is (much?) larger than $\dot{M}_{e,\mathrm{nuc}}$. As M_e decreases below M_{eD} (in this instance $\sim 0.002\ M_\odot$), the radius of the corresponding quasi-static hydrogen-burning model becomes ever more sensitive to the precise value of M_e. Once M_e (and the corresponding radius) shrinks below another critical value ($= M_{eR}$), the mechanism responsible for the ordinary (or super)wind is presumably shut off. If a superwind is responsible for the reduction of M_e to M_{eR}, the extended remnant PNN is probably not in nuclear-burning equilibrium, and it will contract on a thermal time scale (in this instance, measured in hundreds of years) until it reaches a point on the quasi-static track where the rate of evolution is at last controlled by $\dot{M}_{e,\mathrm{nuc}}$.

We have absolutely no idea from first principles as to what the value of M_{eR} should be. However, it has been argued (e.g., Härm and Schwarzschild 1975; Renzini 1979, 1981*a*, 1983) that the total time elapsed between the ejection event and the excitation of the nebula (the transition time τ_{tr}) must typically be less than some fraction of the expansion age of typical PNe or, perhaps, on the order of the expansion age of the smallest and presumably youngest observed PNe (few thousand years). If, for example, we assume in the present instance that $\tau_{\mathrm{tr}} < 5000$ yr, then (from Fig. 1) $M_{eR} < 0.0015\ M_\odot$. If, further, we assume that all high-luminosity PNNi are fueled by hydrogen burning, then, in this instance, a very strong lower limit on remnant envelope mass is $M_{eR} > M_{eF} =$

$2.7 \times 10^{-4}\ M_\odot$. If M_{eR} were comparable to or less than this limit, not only would the transition time drop to just a few hundred years, but so would the lifetime of the entire high luminosity–high surface temperature phase. It seems reasonable that a realistic estimate of M_{eR} is closer to the upper limit of $0.0015\ M_\odot$.

The "fading time" of the PNN, defined as the time for the bolometric luminosity to drop from its plateau value at $T_e \approx 30{,}000$ K to a value 10 times lower while burning hydrogen, is $\tau_{f,\mathrm{H}} \sim 16{,}000$ yr, not unlike expansion lifetimes of typical observed PNe. Note that, using an argument similar to that which produces equation (6), we may estimate

$$\tau_{f,\mathrm{H}} \lesssim \tau_{\mathrm{ip}}(M_{eN} - M_{eF})/\Delta M_{\mathrm{H}} \sim 0.1\tau_{\mathrm{ip}}\ , \qquad (8)$$

which gives $\tau_{f,\mathrm{H}} < 25{,}000$ yr for $M_{\mathrm{H}} = 0.6\ M_\odot$, not terribly much larger than the more carefully obtained result. Using the values of τ_{ip} from Iben (1975*a*, 1977, 1982), we have $\tau_{\mathrm{ip}} \sim 2.5 \times 10^5$ yr $(0.6\ M_\odot/M_{\mathrm{H}})^{10.0}$, and normalizing to $\tau_{f,\mathrm{H}} \sim 16{,}000$ yr when $M_{\mathrm{H}} \sim 0.6\ M_\odot$, we have

$$\tau_{f,\mathrm{H}} \sim 1.6 \times 10^4\ \mathrm{yr}\ (0.6\ M_\odot/M_{\mathrm{H}})^{10.0}\ . \qquad (9)$$

It follows from equation (9) that, for $M_{\mathrm{PNN}} \sim 0.56$–$0.64\ M_\odot$, $\tau_{f,\mathrm{H}} \sim 32{,}000 \rightarrow 8000$ yr. The chosen range in remnant mass encompasses the peak in the observed white dwarf distribution and the range in fading times is comfortably within the range in expansion or "observable" lifetimes of typical PNe; one might therefore be tempted to adopt these coincidences as evidence that most hot, bright PNNi are in an extended hydrogen-burning phase. This is the point of view adopted by Schönberner (1981) and by Schönberner and Weidemann (1983), but other interpretations are possible.

III. PNN EVOLUTION AT CONSTANT MASS—THE CASE OF (NEARLY) PURE HELIUM BURNING

If the AGB phase were *always* terminated by a superwind which sets in when a critical luminosity is exceeded or whose strength is extremely sensitive to luminosity (e.g., producing a mass loss rate proportional to a very high power of L), then one might expect PN ejection to occur preferentially just after a helium shell flash. During a flash, hydrogen burning is extinguished and, as energy produced by helium burning diffuses outward, a significant brightening and increase in radius occurs which lasts for roughly 1% of the interpulse lifetime (or, for about 2500 yr in the current instance). If, during this bright phase, the superwind carries off most of the remaining hydrogen-rich envelope, the resultant PNN might be expected to continue burning helium, but now at very high surface temperatures, for a time comparable to the duration of the quiescent helium-burning phase on the AGB. This duration is on the order of 10% of the interpulse lifetime, or roughly the same as the lifetime of a hydrogen-burning PNN. Thus, purely from considerations of PNN lifetime, one cannot determine whether the superwind occurs only during the bright phase immediately following a helium shell flash, with the ultimate source of ionizing photons from the PNN being primarily helium burning, or whether departure from the AGB occurs at some arbitrary point during the interpulse phase, with the ultimate source of ionizing photons from the PNN being primarily hydrogen burning.

For $M_{\mathrm{PNN}} \sim 0.6\ M_\odot$, we expect a helium-burning lifetime which is on the order of 25,000 yr $(=0.1\tau_{\mathrm{ip}})$. To check this estimate, we choose the $0.6\ M_\odot$ initial model just as it is entering the bright phase following the tenth pulse peak (Iben 1982) and subject it to mass loss at a rate $\dot{M} = -3.33 \times 10^{-6}\ M_\odot\ \mathrm{yr}^{-1}$, arbitrarily calling a halt to mass loss when $M_e = M_{eR} = 0.00060\ M_\odot$ and $M_{\mathrm{PNN}} = 0.5907\ M_\odot$. At this point, the model has $\log T_e = 3.818$, $\log L = 3.756$, and radius $R = 58.3\ R_\odot$. The subsequent evolution is described by the heavy solid track (helium burning) and the thin dashed track (hydrogen burning) in Figure 1. Note that the envelope mass M_e is *constant* during the helium burning phase so that, in contrast to the case of hydrogen burning, the location in the H-R diagram is not uniquely related to M_e but is instead related to the time elapsed since the start of quiescent helium burning.

The helium-burning lifetime of this model PNN as a hot ($T_e > 30{,}000$ K) star is in excess of 40,000 yr, and the following hydrogen-burning lifetime is on the order of 20,000 yr, this latter lifetime being adjustable according to the choice of M_{eR}. The helium-burning lifetime is roughly twice that of a corresponding AGB model, the difference being due to the fact that the PNN model burns at a lower average luminosity than that of the corresponding AGB model. For the same reason, the duration of the final hydrogen-burning phase is larger than that of a model of the same initial envelope mass which has not experienced a helium shell flash as a PNN. The fading time is clearly in excess of 45,000 yr (the precise value being a function of the assumed value of M_{eR}), or almost 3 times that of a PNN which burns only hydrogen. Results to be described in § VI show that, if $M_{eR} \lesssim M_{eF}$, the fading time for pure helium-burning models is approximately

$$\tau_{f,\mathrm{He}} \sim 2.5\tau_{f,\mathrm{H}}\ . \qquad (10)$$

IV. THE CASE OF HELIUM IGNITION IN THE WHITE DWARF CONFIGURATION

We continue the experiments, constructing successively more massive PNNi which are initially in the hydrogen-burning phase. The track followed by a model which has a mass $M_{\mathrm{PNN}} = 0.5995\ M_\odot$, which departs the AGB when $M_e \lesssim 0.002\ M_\odot$, and which continues to burn hydrogen until $M_e = M_{eF} \approx 0.00027\ M_\odot$ is essentially identical to the heavy dashed track in Figure 1 for $\log L \gtrsim 1.8$. However, following the cessation of hydrogen burning, enough of the gravitational energy which is released in the helium-rich zone as a consequence of rapid contraction goes into heating this zone that a final helium shell flash is ignited, even though the mass $\delta M_{\mathrm{H}} = \delta M_{HI} \approx 0.0091\ M_\odot$ added to the helium zone by hydrogen burning following the previous helium shell flash on the AGB is smaller than the comparable mass $\Delta M_{\mathrm{H}} \approx 0.01\ M_\odot$ which accrues between shell flashes for those models of core mass $M_{\mathrm{H}} \sim 0.6\ M_\odot$ that remain on the AGB. In the left-hand panel of Figure 2, only that portion of the track which is followed by the model after helium shell flash ignition is shown.

During the shell flash, the outer edge of the convective zone that appears in the helium-burning region reaches the base of the remaining hydrogen-rich envelope and begins to extend into this envelope, a phenomenon first predicted by Fujimoto (1977) and found in detailed computations by Schönberner (1979). A way of artificially following the subsequent engulfment of the hydrogen-rich layers was

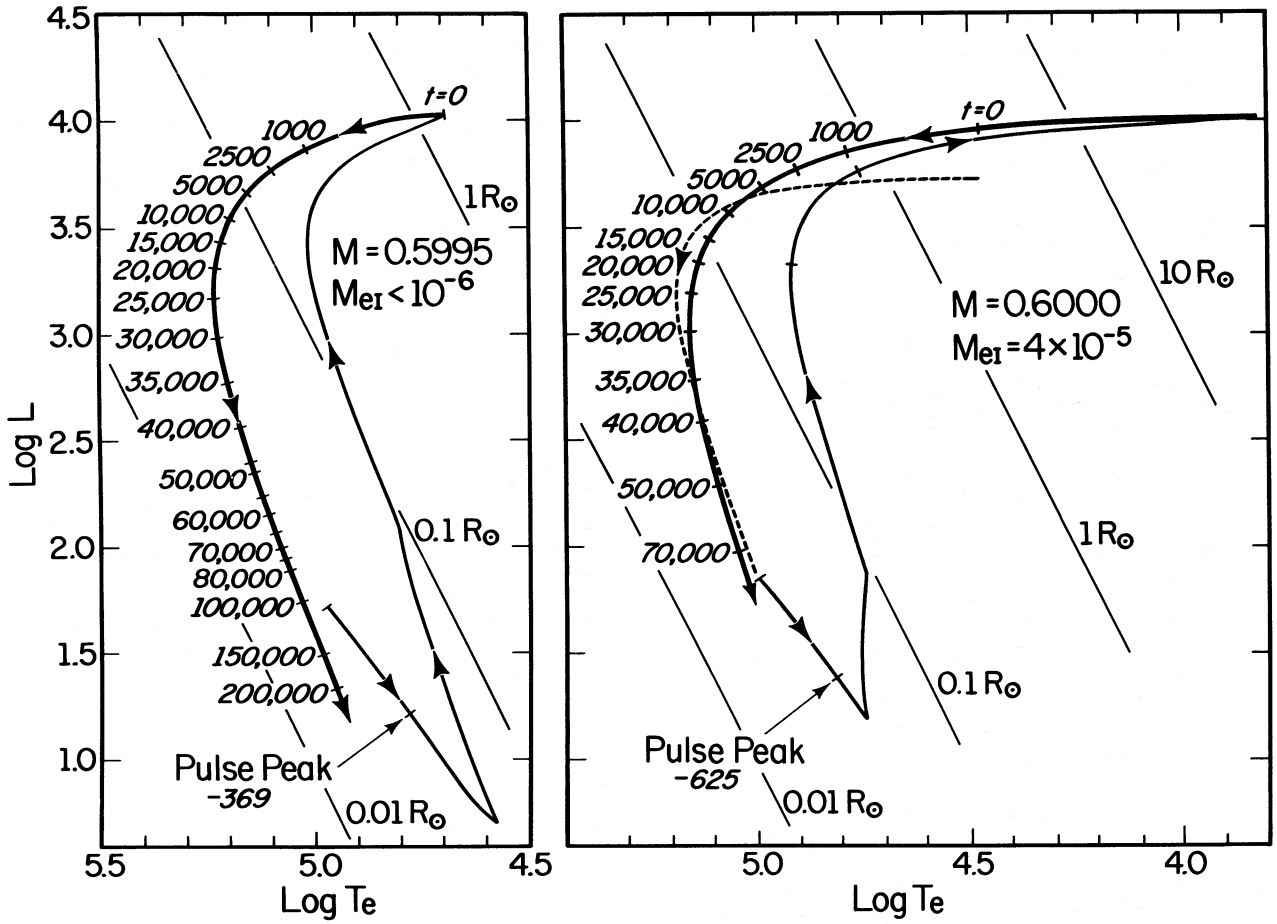

FIG. 2.—Tracks of models which experience a helium shell flash after the hydrogen-burning PNN phase has terminated. The dashed track in the right-hand panel is followed during the preceding hydrogen-burning and initial "cooling" phases while matter in the helium shell is actually heating. In the left-hand panel, model mass $M = 0.5990\ M_\odot$, and the mass in the hydrogen-rich envelope after the peak of the helium-shell flash is $M_{eF} \lesssim 10^{-6}$. In the right-hand panel, $M = 0.6000\ M_\odot$ and $M_{eF} \sim 4 \times 10^{-5}\ M_\odot$. Evolution times are indicated in years, and lines of constant radius are shown for reference.

employed by Iben *et al.* (1983), who concluded that the mass of the hydrogen-rich envelope remaining after pulse peak is considerably smaller than that before pulse peak. For a model of mass $M_{\rm PNN} = 0.6000\ M_\odot$ they found $M_{eF} \sim 4 \times 10^{-5}\ M_\odot$. In the current instance, the same procedure leads to $M_{eF} < 10^{-6}\ M_\odot$. In both instances, the final hydrogen profile is a step function (i.e., there is no hydrogen below the point $M - M_{eF}$).

Even though the procedure used to bypass the extremely complicated physics which occurs during the peak period of the flash is highly artificial, the gross features of the subsequent evolution are expected to be in large part independent of this complicated physics. Thus, the time scales and the evolutionary track following pulse peak are expected to be a reasonable approximation to the truth. As pointed out by Iben *et al.* (1983), the track in the H-R diagram during the quiescent helium-burning phase ($t > 0$ in Fig. 2) is nearly the same as that followed by the model PNN during the preceding high T_e hydrogen-burning phase, and the time scales for evolution along the brightest portions of the tracks for the two phases are comparable (actually ~twice as long for the case of quiescent helium burning).

The near identity of the tracks for the two extended nuclear burning phases is made transparent in the right-hand panel of Figure 2, which depicts evolution in the H-R diagram of the model PNN of mass $M_{\rm PNN} = 0.6000\ M_\odot$ studied by Iben *et al.* (1983). The solid portion of the track is traversed during the helium-burning phase, while the dashed portion of the track is traversed during the hydrogen-burning phase and the following brief gravitational contraction phase. In this case, when the helium shell flash begins, the mass which has been added to the helium zone since the previous thermal pulse on the AGB is $\delta M_{\rm H} = \delta M_{\rm HI} \approx 0.0096\ M_\odot$.

A major feature of this type of evolution is the prediction that the associated PN (whether observable or not) should pass through two phases of high luminosity. Whether or not the second phase is observable depends somewhat on the time elapsed between the two phases. The longer this time delay is, the larger the nebula and the smaller its surface brightness will be during the second phase of high luminosity. In the two cases of double excitation presented here, the duration of the first phase is roughly 16,000–17,000 yr. After approximately 2000 yr of further evolution, during which surface luminosity is due primarily to the release of stored

gravitational potential energy and stored heat, helium is ignited in the shell. The reexcitation of the nebula at high luminosity occurs in another 500 yr or so. Thus, the time elapsed between the two extended nuclear-burning phases is short compared with the duration of each phase, and one expects that, if the first nebular phase is easily observable, the second one is also potentially observable. However, the average linear dimensions of the nebula during the second phase are perhaps 2 to 3 times greater than during the first phase, and the surface brightness will therefore be perhaps 10–30 times smaller. Therefore, in any given observed sample of PNe, those in a possible second phase of illumination may be considerably underrepresented relative to their actual frequency.

Another feature of this type of PNN evolution is that, over the more than 30,000 yr duration of the second high-luminosity phase, only a modest wind from the hot central star (for the two cases studied, $\dot{M} \sim -5 \times 10^{-11}\ M_\odot\ \mathrm{yr}^{-1}$ and $\dot{M} \sim -2 \times 10^{-9}\ M_\odot\ \mathrm{yr}^{-1}$) is necessary to remove whatever vestiges of hydrogen-rich material remain at the surface following the helium shell flash. These modest rates are smaller than typical observational estimates (Heap 1979, 1980; Perinotto, Benvenuti, and Cacciari 1981; Castor, Lutz, and Seaton 1981), and one is encouraged to hope that we understand how at least some non-DA white dwarfs come into being.

V. THE CASE OF HELIUM SHELL FLASH IGNITION IN CENTRAL STARS OF HIGH LUMINOSITY

The addition of just $\sim 0.0004\ M_\odot$ to the model PNN of mass $M_{\mathrm{PNN}} = 0.6000\ M_\odot$ is sufficient to allow the core mass M_{H} to grow during the high-luminosity phase of hydrogen burning ($M_e \gg M_{eF}$) until $\delta M_{\mathrm{H}} \approx \Delta M_{\mathrm{H}}$, the critical increment in helium zone mass which brings about a helium shell flash in an AGB star. Thus, as shown in Figure 3, a model PNN of mass $M_{\mathrm{PNN}} = 0.6005\ M_\odot$ experiences a helium shell flash before hydrogen burning ceases. The mass in the envelope when this occurs is $M_{eI} = 0.00047\ M_\odot$. Along the track in Figure 3, time is measured from the point at which the model achieves $T_e = 30{,}000$ K while burning helium on a long time scale. As in the case when helium shell flash ignition occurs after the cessation of hydrogen burning, the associated PN will experience two phases of high-luminosity excitation. The first phase, when the exciting photons are due to hydrogen burning (the luminous, heavy-dashed portion of the track), lasts for roughly 11,000 yr (14,500 – 3240) and the second phase, when the exciting photons are due to helium burning (the heavy, solid portion of the track), lasts approximately

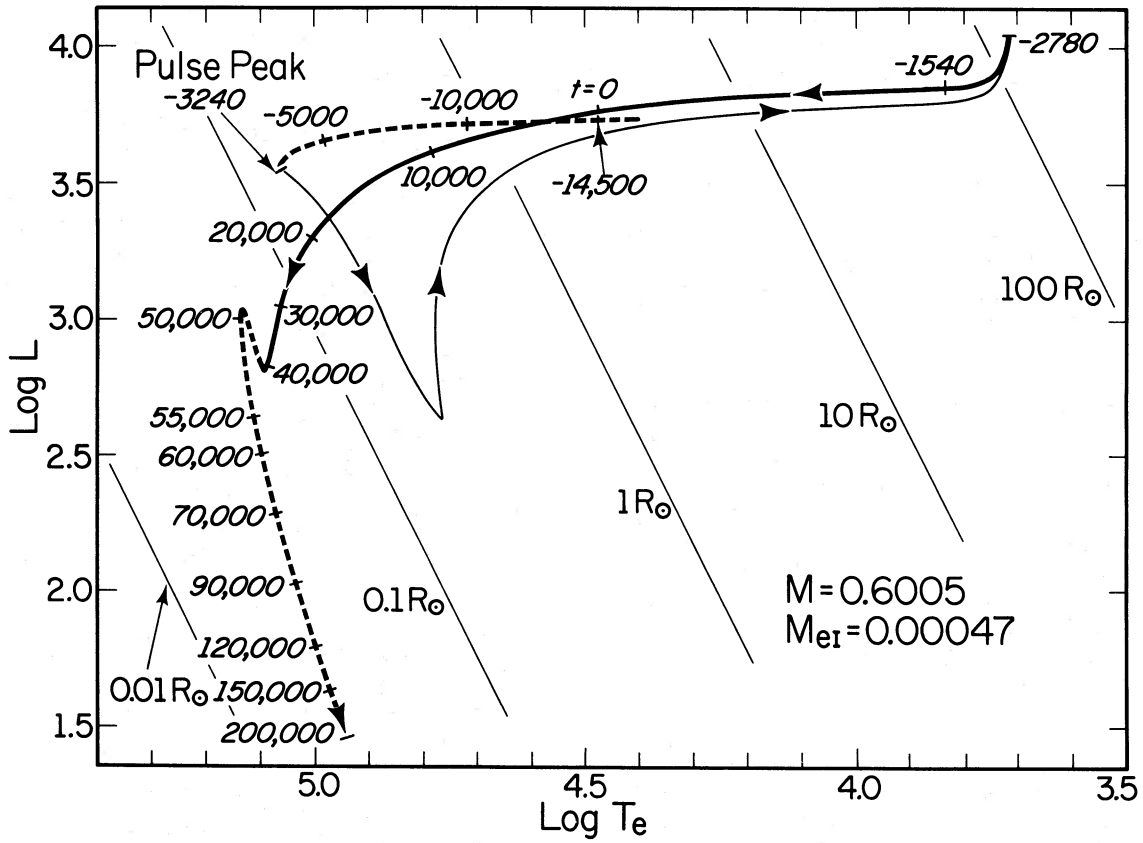

FIG. 3.—Evolutionary track of a model of mass $M = 0.6005\ M_\odot$ which experiences a helium shell flash (thermal pulse) during the luminous portion of the hydrogen-burning phase (*upper dashed track*) when the mass in the hydrogen-rich envelope is $M_{eI} = 0.00047\ M_\odot$. Hydrogen burning is shut off during the sharp dip immediately following pulse peak, and helium burning provides most of the surface luminosity along the solid portion of the track until hydrogen is rekindled briefly at $t \sim 40{,}000$ yr. Hydrogen burning effectively ceases by $t \sim 55{,}000$ yr when $M_e = M_{eF} \sim 0.00027\ M_\odot$. Along the rest of the dashed track, surface luminosity is provided by outward leakage of thermal energy. Times are indicated in years and lines of constant radius are shown for reference.

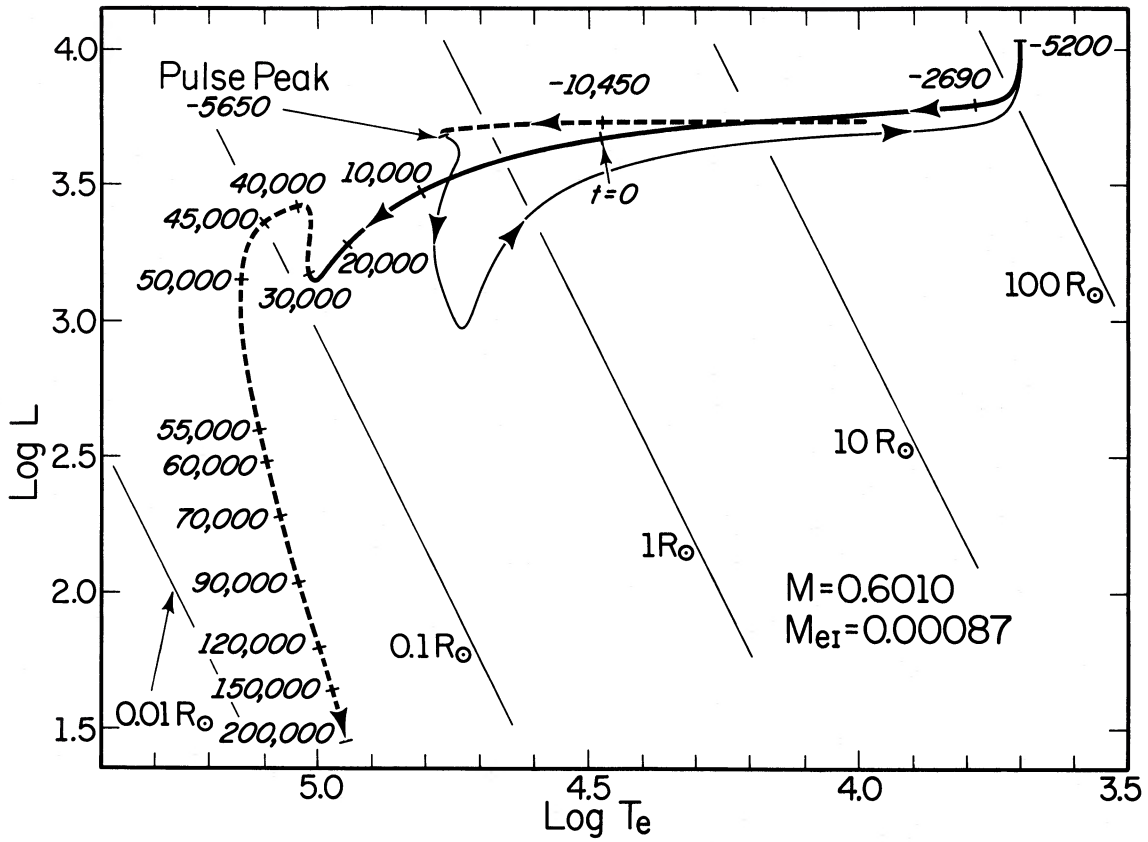

FIG. 4.—Same as Fig. 3 for a model of mass $M = 0.6010\ M_\odot$ which experiences a helium shell flash while hydrogen burning when $M_{eI} = 0.00087\ M_\odot$

40,000 yr. The two phases are separated by about 3000 yr, much of which the PNN spends as a red giant. Near the terminus of the solid portion of the track, hydrogen reignites and burns for about 10,000 yr as the envelope mass is reduced from $4.7 \times 10^{-4}\ M_\odot$ to $2.7 \times 10^{-4}\ M_\odot$ (the light, dashed portion of the track).

The rate at which the PNN dims after the cessation of the final hydrogen-burning phase is considerably smaller than when a helium shell flash does not interrupt the process of hydrogen burning (see Fig. 1). The time for the PNN to dim from $\log L \sim 2.7$ to $\log L \sim 1.7$ is roughly 90,000 yr in the case of interruption and is only about 30,000 yr when no interruption occurs. The difference is due simply to the fact that nuclear burning in the helium-rich zone maintains this zone at high temperatures, and it is the leakage outward of heat stored in this zone that maintains the flash-experiencing PNN at a relatively high luminosity for some time after active nuclear burning has ceased. This phenomenon is also evident on comparing evolutionary times along the dashed and solid tracks in Figure 1.

Of possibly high significance is the fact that, during the brightest luminosity portion of the quiescent helium-burning phase, the PNN returns to the AGB and remains there for some time (~ 1000 yr) even though the mass in the envelope is far too small to allow the star to remain there if surface luminosity were supplied primarily by quiescent hydrogen burning. It is to be expected that any wind which operates during the preceding AGB phase will be reactivated during this second sojourn as an AGB star.

Additional examples of model PNNi that burn fuel alternately in two shells are shown in Figures 4 and 5. The notation in these two figures has the same significance as in Figure 3: $t = 0$ is the point at which the associated PN is excited at the beginning of an extended phase of helium burning (*solid track*); the high-luminosity dashed portion of the curve is the track followed during the first hydrogen-burning phase; and the first part of the dashed curve which appears after the terminus of the solid curve is the track followed during the second hydrogen-burning phase. Several PNN characteristics for the three morphologically equivalent cases represented in Figures 3–5 are given in Table 1. Masses in this table are in solar units and times are in years. Further, $\tau_{H1}(\tau_{H2})$ = lifetime of that portion of the first (second) hydrogen-burning phase when $T_e > 30{,}000$ K; τ_{He} = lifetime of the helium-burning phase when $T_e > 30{,}000$ K; and τ_{RG} = time spent as a red giant with stellar radius $R \gtrsim 0.5 R_{max}$, where R_{max} is the maximum radius attained by the star ($\sim 150\ R_\odot$ in the three cases).

In Figure 6 is shown the result of increasing model mass (to $M_{PNN} = 0.6025\ M_\odot$) so that the last helium shell flash is initiated while the model is still on the AGB. Remarkably, even though M_e remains constant and large during the ensuing helium-burning phase ($M_e = 0.00238$), the model departs from the AGB not only during the phase of rapid luminosity variations immediately following pulse peak (the sharp dip and sharp rise referred to in Iben 1982)

TABLE 1

PROPERTIES OF MODEL PNNi WITH MULTIPLE BURNING PHASES

M_{PNN}	M_{eI}	τ_{H1}	τ_{He}	τ_{H2}	τ_{RG}	M_{eI}/τ_{RG}
0.6005	0.00047	11,000	30,000	10,000	1240	−3.8/−7
0.6010	0.00087	5000	30,000	20,000	2510	−3.5/−7
0.6015	0.00136	0	30,000	30,000	3720	−3.7/−7
0.6025	0.00238	0	10,000	48,000	6700	−3.6/−7

but eventually also toward the latter portions of the subsequent extended quiescent helium-burning phase. More remarkably still, the model does not return to the AGB after helium burning dies down and hydrogen is rekindled, even though the envelope mass is initially too large to permit a model already in the midst of a quiescent hydrogen-burning phase to depart from the AGB. It is to be expected that, in the real analog, wind mass loss will continue to reduce M_e and accelerate the departure from the AGB which the constant mass model undertakes of its own volition. Similar results have been obtained by Gingold (1974, 1976). Inserting relevant characteristics of the 0.6025 $M_\odot$ model PNN in Table 1, we now embark on a speculative journey.

VI. THE OCCURRENCE OF A SECOND PN EJECTION EVENT AND ITS CONSEQUENCES

The fact that, in all four cases discussed in § V, τ_{RG} is almost exactly proportional to M_{eI} may provide the clue to understanding how perhaps one-half to two-thirds of all non-DA white dwarfs (with $T_e > 12{,}000$ K) achieve their hydrogen-free surfaces. The mass loss rate defined by $-M_{eI}/\tau_{RG}$ is in all four cases detailed in Table 1 approximately $\dot{M}_e \sim -3.6 \times 10^{-7}\, M_\odot\ \mathrm{yr}^{-1}$. This is less than twice as large as the mass loss rate given by the Reimers expression with $\eta = \frac{1}{3}$ when $L \sim 8 \times 10^3\ L_\odot$, $R \sim 125\ R_\odot$, and $M \sim 0.6\ M_\odot$. That is, a mass loss rate only slightly larger than that of the "ordinary" wind which AGB stars are thought to experience is sufficient to remove much of the hydrogen-rich envelope with which a model PNN returns to the AGB immediately following a flash that either is initiated far from the AGB (Figs. 3–5) or drives the star far from the AGB during the extended helium luminosity "dip" phase (Fig. 6).

Of course, an ordinary wind cannot succeed in removing all of the envelope, since, at any given L, the radius of a quasi-static model decreases with decreasing M_e and, as we have just seen, the time which a constant-mass model spends as a "born-again" AGB star decreases linearly with decreasing M_e. Thus, if only an ordinary wind operates, a substantial portion of the envelope must remain as the model departs from the AGB for a second time.

If, however, a superwind of sufficient strength causes the first departure from the AGB, then, when this wind is reactivated, significantly more envelope mass may be lost than in the case of loss by an ordinary wind. A first estimate of how much mass may be lost by a superwind during the

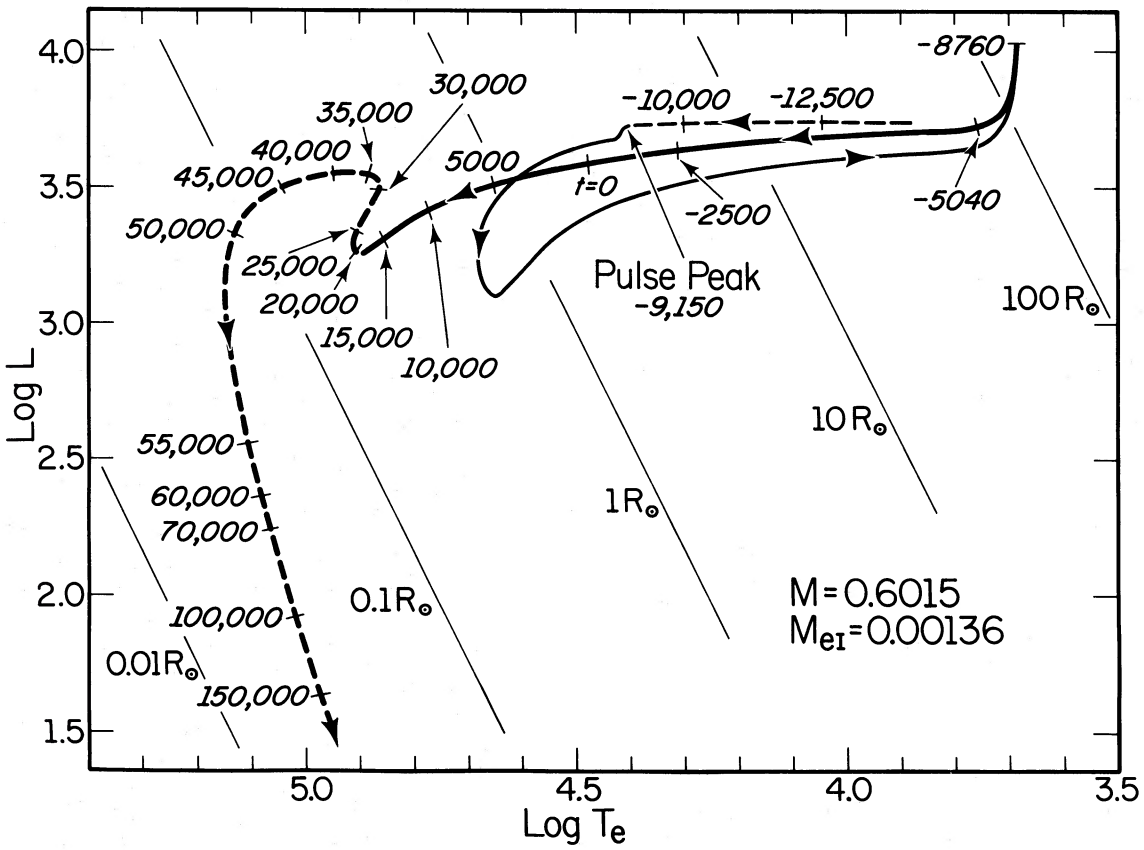

FIG. 5.—Same as Fig. 3 for a model of mass $M = 0.6015\ M_\odot$ which experiences a helium shell flash while hydrogen burning when $M_{eI} = 0.00136\ M_\odot$

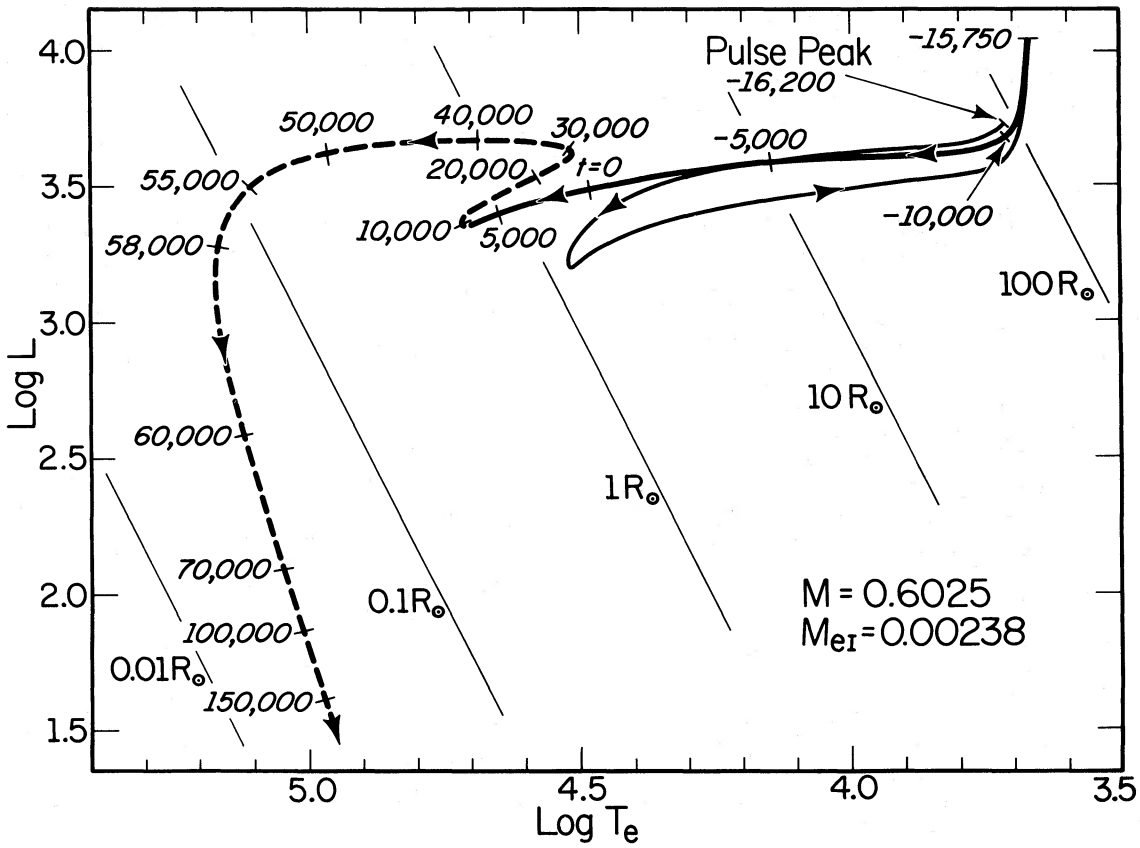

FIG. 6.—Same as Fig. 3 for a model of mass $M = 0.6025\ M_\odot$ which experiences a helium shell flash while hydrogen burning on the AGB when $M_{eI} = 0.00218\ M_\odot$.

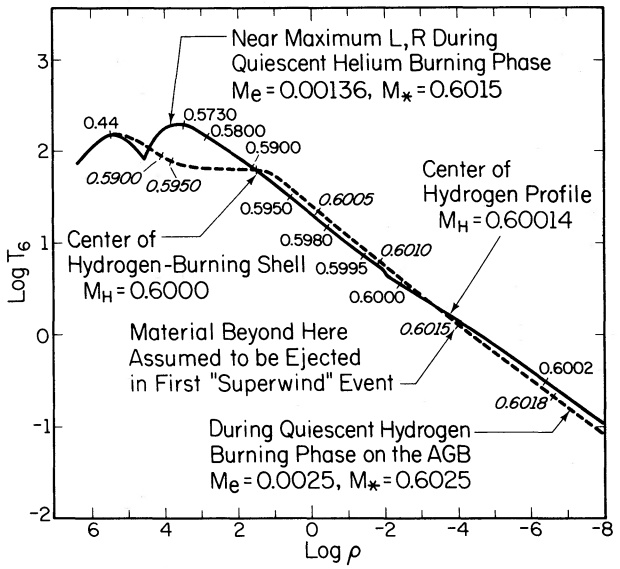

FIG. 7.—Density (g cm^{-3}) – temperature (10^6 K) relationships for matter in two model stars: (1) an AGB star (*dashed curve*) of total mass $M = 0.6025\ M_\odot$, "core" mass $M_H = 0.6000\ M_\odot$, and envelope mass $M_e = 0.0025\ M_\odot$; and (2) a "born-again" AGB star (*solid curve*) with $M = 0.6015\ M_\odot$, $M_H = 0.60014\ M_\odot$, and $M_e = 0.00136\ M_\odot$. The associated mass coordinate is indicated in solar units beside each tick mark.

born-again AGB phase follows from a comparison of conditions in the envelope of the born-again star with those in the envelope of a possible hydrogen-burning AGB precursor. In Figure 7, the variation of ρ and T is shown for a hydrogen-burning AGB model of total mass $M = 0.6025\ M_\odot$ and core mass $M_H = 0.6000\ M_\odot$ (located in the H-R diagram essentially at the point marked "Pulse Peak" in Fig. 6) and for the born-again, helium-burning AGB model of total mass $M = 0.6015\ M_\odot$ (located in the H-R diagram at the largest L, lowest T_e point on the track in Fig. 5). In this second model the center of the hydrogen profile is at $M = 0.60014\ M_\odot$. It is evident that, during the highest luminosity portion of the born-again AGB phase, the relationship between density and temperature and/or pressure and density through the envelope (beginning at a point well below the base of the hydrogen-rich region and extending to the surface) is nearly the same as that which obtains during the preceding quiescent hydrogen-burning phase through the envelope (extending outward beyond the center of the hydrogen-burning shell). One might anticipate that, if a superwind strips the precursor star down to the point $M \sim 0.6015\ M_\odot$, where density $\rho \sim 10^{-4}$ and temperature $T \sim 10^6$ K, this same wind would also strip the born-again AGB star down to the point $M \sim 0.60015$, where ρ and T are the same.

Let us carry this thought a bit further. The distribution in ρ and T in a star of the same core mass but of total mass considerably larger than that of the $0.6025\ M_\odot$ model

looks essentially like the distribution for the 0.6025 $M_\odot$ model in the region $M < 0.6015\ M_\odot$. Let us envision a star of initial main-sequence mass about 1.2 $M_\odot$ which, after losing $\sim 0.3\ M_\odot$ during the RG and E-AGB phases via an ordinary wind, reaches the TP-AGB phase with a core mass $M_H \sim 0.53\ M_\odot$ and a total mass $M \sim 0.9\ M_\odot$. After integrating equation (5) with $\eta = \frac{1}{3}$, one derives that continued mass loss via an ordinary wind brings the star to the point where $M_H \sim 0.599\ M_\odot$ with a total mass $M \sim 0.8\ M_\odot$. Since $\tau_{ip} \sim 2.5 \times 10^5$ yr and $\Delta M_H \sim 0.01\ M_\odot$, the star will have spent roughly $\sim 2.2 \times 10^6$ yr in the TP-AGB phase.

Now let a superwind set in and remove mass at the rate $\dot{M}_{SW} \sim -10^{-5}\ M_\odot\ \mathrm{yr}^{-1}$ until $M = 0.6015\ M_\odot$. Over the 2×10^4 yr duration of this episode, the core mass will have grown by about 0.001 $M_\odot$ to 0.600 $M_\odot$ and the envelope mass will have been reduced to $M_e \sim 0.0015\ M_\odot$. Toward the end of the superwind episode, the remnant star must therefore begin to move on a thermal time scale to the position $\log T_e \sim 4.0$, $\log L \sim 3.74$ in Figure 5. Then, after evolving to the blue for another 3000 yr or so, still burning hydrogen quiescently, our hypothetical star experiences a helium shell flash and returns once again to the AGB where, we suppose, the superwind sets in again. As already indicated, the second phase of stripping might be expected to remove matter down almost to the center of the hydrogen profile. A similar scenario follows if the superwind is a milder one, with $\dot{M}_{SW} \sim -10^{-6}\ M_\odot\ \mathrm{yr}^{-1}$, say, and the highest density portion of the nebula-to-be is at a mass much less than 0.2 $M_\odot$ below the surface.

It is worth exploring whether or not quasi-static calculations can reproduce this speculative behavior. We conduct three experiments, beginning with the born-again AGB model of mass 0.6015 $M_\odot$, just as its radius reaches 100 $R_\odot$ for the first time after it has experienced its last helium shell flash. In each experiment, we adopt a constant mass loss rate ($\dot{M} = -10^{-6}\ M_\odot\ \mathrm{yr}^{-1}$ in two instances and $-10^{-5}\ M_\odot\ \mathrm{yr}^{-1}$ in the other) and follow the subsequent evolution until stellar radius again drops below 100 $R_\odot$. The resulting values of $R_e = (M_{eI} - M_e)/M_{eI}$ are taken as a measure of the fractional reduction in envelope mass resulting from the second superwind phase. At this point the three experiments diverge. In the first case, mass loss at the same rate ($-10^{-6}\ M_\odot\ \mathrm{yr}^{-1}$) is maintained until the helium- and carbon-rich layers are exposed, after which $\dot{M} = 0$. In the other two cases, in order to simulate the cessation of a superwind and the onset of a hot wind of reasonable strength, mass loss is set equal to zero until $T_e \geq 30{,}000$ K, and thereafter $\dot{M} = -10^{-8}\ M_\odot\ \mathrm{yr}^{-1}$.

Results of the first experiment are shown in Figure 8. The

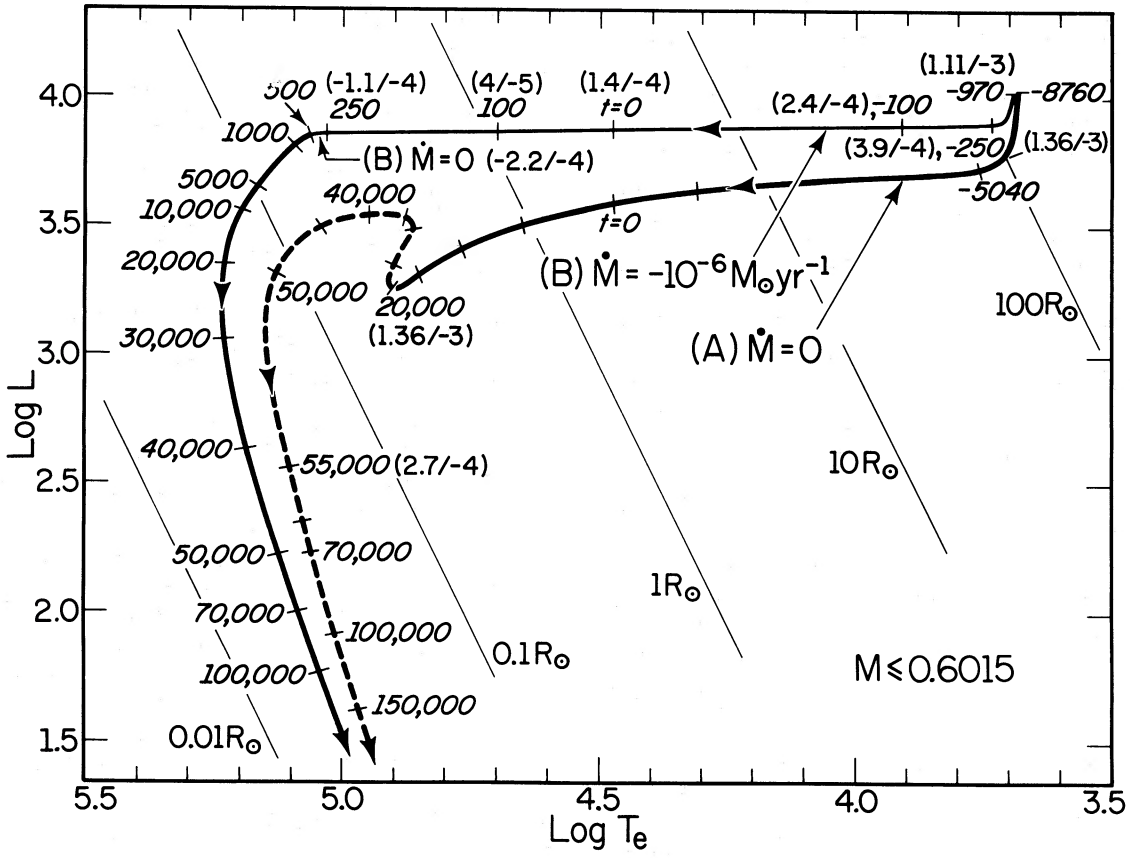

FIG. 8.—Tracks for two models burning helium. Track A is for a model of constant mass $M = 0.6015\ M_\odot$ (copy from Fig. 5), and track B is the result of abstracting mass at the rate $\dot{M} = -10^{-6}\ M_\odot\ \mathrm{yr}^{-1}$ from a model whose mass is initially $M = 0.6015\ M_\odot$. When it first reaches $R = 100\ R_\odot$ (at $t \sim -1220$ yr) during its second ascent of the AGB after experiencing a helium shell flash far to the blue of the AGB (Fig. 5). Mass loss along track B is terminated at $t \sim 290$ yr, when all hydrogen has been lost from the surface. All evolution times are in years, and the mass in the hydrogen-rich envelope (down to the center of the hydrogen profile) is indicated in solar units (in parentheses).

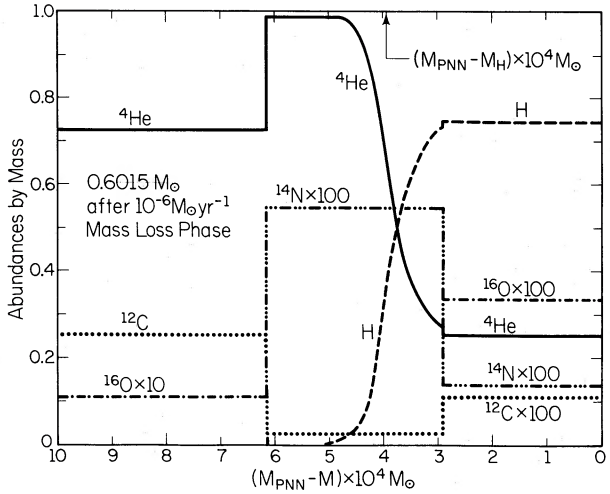

FIG. 9.—Abundances by mass of ^{1}H, ^{4}He, ^{12}C, ^{14}N, and ^{16}O near the outer edge of the PNN shown in Fig. 8 at the point $t = -250$ (or at the point $t = 1160$ in Fig. 10). The horizontal axis is measured in units of $10^{-4}\ M_\odot$ from the surface. In the region containing products of pure hydrogen burning [$M_{PNN} - M \approx (2.9\text{–}6.1) \times 10^{-4}\ M_\odot$] the abundance by mass of ^{16}O increases inward from $\sim 3.3 \times 10^{-6}$ to $\sim 4.0 \times 10^{-6}$.

track marked A($\dot{M} = 0$) is simply a copy of that portion of the track in Figure 5 after the point of maximum L and minimum T_e. To achieve the track marked B($\dot{M} = -10^{-6}\ M_\odot\ yr^{-1}$), the $M = 0.6015\ M_\odot$ model has been subjected to mass loss at the indicated rate, beginning with a point during the second ascent of the AGB following the peak of the helium shell flash ($\log L = 3.765$, $\log T_e = 3.703$, $R = 100\ R_\odot$, $M_e = 0.00136\ M_\odot$). Values of M_e are given in parentheses (in $M_\odot$) beside model times (in yr).

The mass-losing model achieves peak luminosity in about 250 yr at $t \sim -970$ yr, with $\log L \sim 4.03$, $\log T_e \sim 3.693$, $R \sim 142\ R_\odot$, $M \sim 0.6012\ M_\odot$, and $M_e = 0.00111\ M_\odot$. In another 720 yr, at $t \sim -250$ yr, when stellar radius again reaches $\sim 100\ R_\odot$, total stellar mass has been reduced to $M \sim 0.6005\ M_\odot$, and envelope mass has been reduced to $M_e \sim 0.00039\ M_\odot$. Thus, helium burning is able to sustain the model at radii larger than $\sim 100\ R_\odot$ while envelope mass is reduced to less than one-quarter of the value which leads to departure from the AGB during the quiescent hydrogen-burning phase. The fraction by which envelope mass has been reduced during the born-again AGB phase is approximately $R_e = (0.00136 - 0.0039)/0.00136 \sim 0.7$.

It is important to note that the chosen value of $\dot{M}$ is only about twice the Reimers rate with $\eta \sim 1$. Hence, even an "ordinary" wind will remove a substantial portion of the hydrogen-rich envelope during the peak luminosity phase of a born-again AGB star. Another lesson from the experiment described in Figure 8 is that mass loss at the chosen rate forces the model to depart from the AGB before helium-rich layers are exposed. Relevant abundances by mass near the surface of the star when $t = -250$ are shown in Figure 9. The flat profiles for all elements in the envelope for values of $M_{PNN} - M \gtrsim 2.9 \times 10^{-4}\ M_\odot$ is due to the extension of envelope convection inward beginning at the point marked "dredge-up begins" in Figure 10 and continuing until $L = L_{max}$. The hydrogen profile extends in either direction from the point marked $M_{PNN} - M_H$ by about $0.00009\ M_\odot$. In particular, the hydrogen abundance by mass does not drop below 0.01 until the point $M = M_H - 0.00009\ M_\odot$. The edge of the carbon-rich region is not reached until the point $M = M_H - 0.00022\ M_\odot$. In the current instance, then, the hydrogen-rich layers are not completely abstracted until the model reaches a position ($T_e > 30{,}000$ K, $R \lesssim 3\ R_\odot$) quite far from the AGB. Note finally that, even if mass loss were terminated when R falls below $100\ R_\odot$, the duration of the final hydrogen burning phase (which ceases when $M_e < 2.7 \times 10^{-4}\ M_\odot$) would be considerably curtailed.

The post-AGB portion of the formal mass-losing phase ($t = -250$ yr to $t \sim 300$ yr) may be interpreted in the following way. Had we adopted a more robust superwind (as in an experiment yet to be described), we would have achieved a smaller value of M_e by the time stellar radius drops below $\sim 100\ R_\odot$. Thus, the time to evolve to a given position (and a given value of M_e) along the actually computed track in Figure 8 may be viewed as an upper limit to the time required to reach that point by another model which (thanks to a stronger wind) has achieved the given value of M_e while still on the AGB at large radius. Mass loss along track B is continued until the underlying helium- and carbon-rich layers have been exposed ($M_e \sim -0.00022\ M_\odot$) and is then abruptly stopped. The subsequent evolution [after the point B($\dot{M} = 0$)] is appropriate for a non-DA white dwarf progenitor.

A possibly more realistic variant of PNN evolution during helium-burning phases is described in Figure 10. Here, the entire PNN evolutionary track, including that traversed during the initial hydrogen-burning phase, is shown. Time is measured from the moment of pulse peak rather than from the moment when $T_e \gtrsim 30{,}000$ and, again, $M_e/M_\odot$ is given in parentheses. Further, $\dot{M} = 0$ until $R \sim 100\ R_\odot$, $t = 190$ yr; $\dot{M} = -10^{-6}\ M_\odot\ yr^{-1}$ for $R \gtrsim 100\ R_\odot$; $\dot{M} = 0$ for $R < 100\ R_\odot$ and $T_e < 30{,}000$ K; $\dot{M} = -10^{-8}\ M_\odot\ yr^{-1}$ for $T_e > 30{,}000$ K and $\log L > 2.0$; and $\dot{M} = 0$ for $\log L < 2.0$. Thus, the low-velocity "modest superwind" is constrained to operate at large radii and the fast "hot wind" is constrained to operate at high temperature and high luminosity.

On comparing Figures 8 and 10 it is clear that, in the case of continued mass loss at a high rate, evolution to the blue following the born-again AGB phase is completely controlled by the steady reduction in M_e; in the case when $|\dot{M}| \leq 10^{-8}\ M_\odot\ yr^{-1}$ for $R \lesssim 100\ R_\odot$, evolution to the blue is controlled by structural changes engendered by modifications in the helium-burning rate. After some 48,000 yr of mass loss via the adopted hot wind, the surfaces of the model PNN becomes hydrogen free. After a further 13,000 yr of evolution, the edge of the carbon- and helium-rich region that has been left behind by the convective shell during the last helium shell flash is exposed. Since one might expect that the strength of the hot wind decreases as luminosity decreases, the possibility arises that, in some real analogs, the exposure of highly processed layers ceases shortly after the hydrogen-free (and also essentially carbon-free) layer is reached. By the same token, in some cases, exposure may not even extend to the hydrogen-free layer. It seems reasonable to suppose that the fractional reduction in envelope mass that occurs during the second superwind stage is, in first approximation, independent of M_{eI}. It follows that, the smaller M_{eI} is to begin with, the deeper are the layers which are ultimately exposed during the fast, hot wind stage.

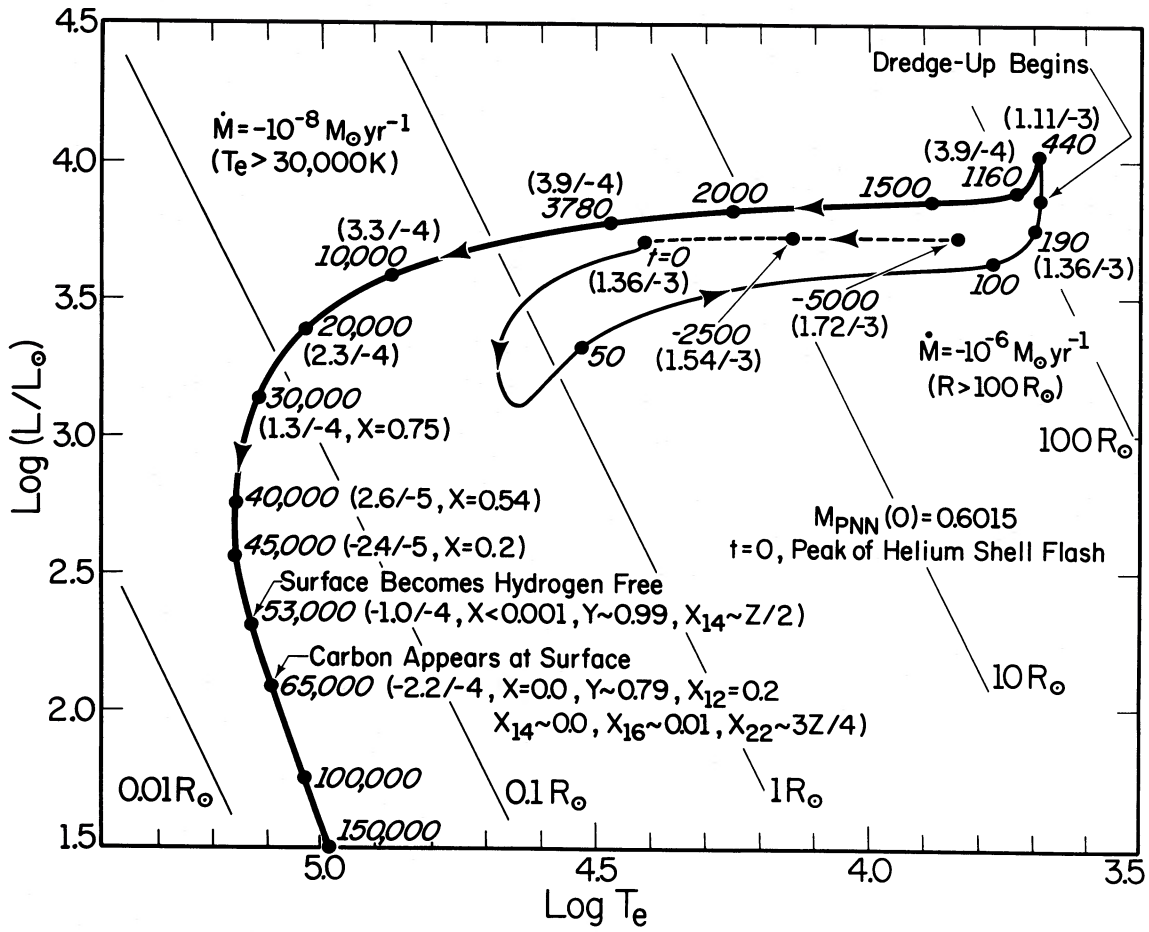

FIG. 10.—Evolutionary track of a model PNN which is subjected to mass loss at the rate $\dot{M} = -10^{-6}\ M_\odot$ yr during the born-again AGB phase while $R \geq 100\ R_\odot$. When radius drops below 100 $R_\odot$ and until $T_e = 30{,}000$ K, $\dot{M} = 0$. When T_e exceeds 30,000 K, mass loss via a postulated hot wind is initiated at the rate $\dot{M} = -10^{-8}\ M_\odot\ \mathrm{yr}^{-1}$ and, when $\log L \leq 2.0$, mass loss is again terminated. Time is measured from the moment that the helium-burning luminosity reaches its peak during a final helium shell flash. The times to reach various locations on the track are given (in years), and the mass in the envelope above the center of the hydrogen profile is given in parentheses beside each time. Also in parentheses along that portion of the track during which $\dot{M} = -10^{-8}\ M_\odot\ \mathrm{yr}^{-1}$ is given the surface abundances by mass of hydrogen (X), helium (Y), ^{12}C (X_{12}), ^{14}N (X_{14}), ^{16}O (X_{16}), and ^{22}Ne (X_{22}).

Results of the final experiment are shown in Figure 11. The only difference from the experiment described in Figure 10 is that $\dot{M} = -10^{-5}\ M_\odot\ \mathrm{yr}^{-1}$ while $R > 100\ R_\odot$. After completion of the final superwind episode, envelope mass has been reduced to $M_e = 8.9 \times 10^{-5}\ M_\odot$, and the initial rapid evolution to the blue (from $t = 313$ to $t \sim 550$) proceeds at about the same rate as does the evolution of the mass-losing model described in Figure 8 up the position at which M_e is reduced to $9 \times 10^{-5}\ M_\odot$ (from $t \sim -250$ to $t \sim 50$). Thereafter, evolution to the blue proceeds at a considerably reduced rate. After mass loss via a hot wind (again at a rate $\dot{M} = -10^{-8}\ M_\odot\ \mathrm{yr}^{-1}$) has continued for approximately 19,000 yr, the outer edge of the hydrogen-free, carbon-poor layer is exposed, and after a still further 12,000 yr of mass loss, the outer edge of the carbon-rich, helium-rich layer is exposed.

Summarizing results of the three mass loss experiments, it is evident (and obvious) that, the higher the mass-loss rate is during the born-again AGB phase and the longer this high rate can be maintained, the more effective is the hot wind in exposing highly processed layers during the subsequent high-luminosity, high surface temperature helium-burning phase. However, it does not appear that the superwind is by itself capable of exposing hydrogen-free layers, and it is therefore difficult to understand how these models relate to R CrB stars, a difficulty which will be discussed further in § VIII.

VII. ON THE PROBABILITIES OF VARIOUS EVOLUTIONARY PATHS AND PREDICTIONS ABOUT WHITE DWARF SURFACE CHARACTERISTICS

In the absence of any meaningful theoretical guidance, we must adopt various assumptions concerning the probability that a star will depart from the AGB at any given *phase* of its nuclear burning cycle and then examine the consequences. In this section, we shall pretend that all PNNi are of mass $\sim 0.6\ M_\odot$, but each result is presented in such a way as to hopefully be valid for every PNN mass. In particular, estimates of probabilities are assumed to be, in first approximation, independent of PNN mass. As a first example, suppose that, over the duration of a single cycle, the mass loss rate is relatively constant, independent of phase. Then, the probability of departure from the AGB is also independent of phase. The fraction of stars that first depart from the

AGB during the hydrogen-burning phase will be proportional to the duration τ_H of this phase and the fraction that first depart during helium burning phases will be proportional to the duration τ_{He} of these phases. Since $\tau_{He} \sim 0.1\tau_{ip}$ and $\tau_H \sim 0.9\tau_{ip}$, we have that 90% leave while burning hydrogen and 10% leave while burning helium. Those stars that leave while burning helium will not return to the AGB. What happens to those that leave while burning hydrogen depends on the precise phase in the hydrogen-burning cycle when departure occurs. Let us measure this phase by $\phi = \delta M_{HD}/\Delta M_H$, where ΔM_H is the mass eaten through by the hydrogen-burning shell between pulses on the AGB and δM_{HD} is the mass eaten through by the shell since the last pulse before departure from the AGB. If we choose (somewhat arbitrarily) $M_{eD} \sim 0.0015\ M_\odot$ and note that $M_{eN} \sim 0.0012\ M_\odot$, then $\delta M_{HD} \approx \delta M_{HN} - 0.0003\ M_\odot$. From the data presented in § II it may be deduced that, for all values of ϕ less than $0.77 - 0.03 = 0.74$ ($M_{PNN} = 0.5990\ M_\odot$), stars which depart from the AGB do not experience another helium shell flash and thus do not become born-again AGB stars.

Pertinent data for models which experience a helium shell flash after leaving the AGB are displayed in Figure 12. All quantities in this figure have been defined in § II. For values of ϕ between 0.79 ($M_{PNN} = 0.5995\ M_\odot$) and 0.84 ($M_{PNN} = 0.6000\ M_\odot$), a helium shell flash occurs in the white dwarf configuration, after hydrogen burning has ceased. Let us declare these models to be in the type II category, and place in the type I category those models which do not experience a shell flash after departing from the AGB while burning hydrogen. For ϕ greater than 0.89 ($M_{PNN} = 0.6010$), models experience a helium shell flash during hydrogen burning and hence are not of type II. From the curves in Figure 12, we may estimate the upper limit on ϕ for which a contraction-generated flash occurs to be 0.875; a not unreasonable estimate for the total range of type II models is $\Delta\phi_{II} \sim (0.775 \rightarrow 0.875) = 0.1$.

If we assign models which experience a helium shell flash while burning hydrogen at high luminosity and at surface temperatures greater than $T_e = 30{,}000$ K to the type III category, it follows from Figure 10 that $\Delta\phi_{III} \sim 0.97 - 0.875 \sim 0.1$. The $\Delta\phi$ ranges which we have thus far estimated are actually independent of the assumed relationship between δM_{HD} and δM_{HN}, as long as $\delta M_{HD} < \delta M_{HN}$.

Defining the model stars which experience a helium shell flash when $T_e < 30{,}000$ K, but when $M_{eI} < M_{eD}$ as type IV models, we have $\Delta\phi_{IV} \sim 0.03$. We call models which depart from the AGB while burning helium at high luminosity following a helium shell flash type V models. Since the duration of the bright post-flash phase is typically 10% of the duration of the entire helium-burning phase or about 1% of the duration of the total interpulse phase, our assumption of constant $\dot{M}$ over a pulse cycle means that $\Delta\phi_V \approx 0.01$.

Calling models which depart from the AGB during the extended quiescent helium-burning phase type VI models and redefining the $\Delta\phi$'s as probabilities (Ps) by normalizing to the entire interpulse lifetime, we have the entries in the first row

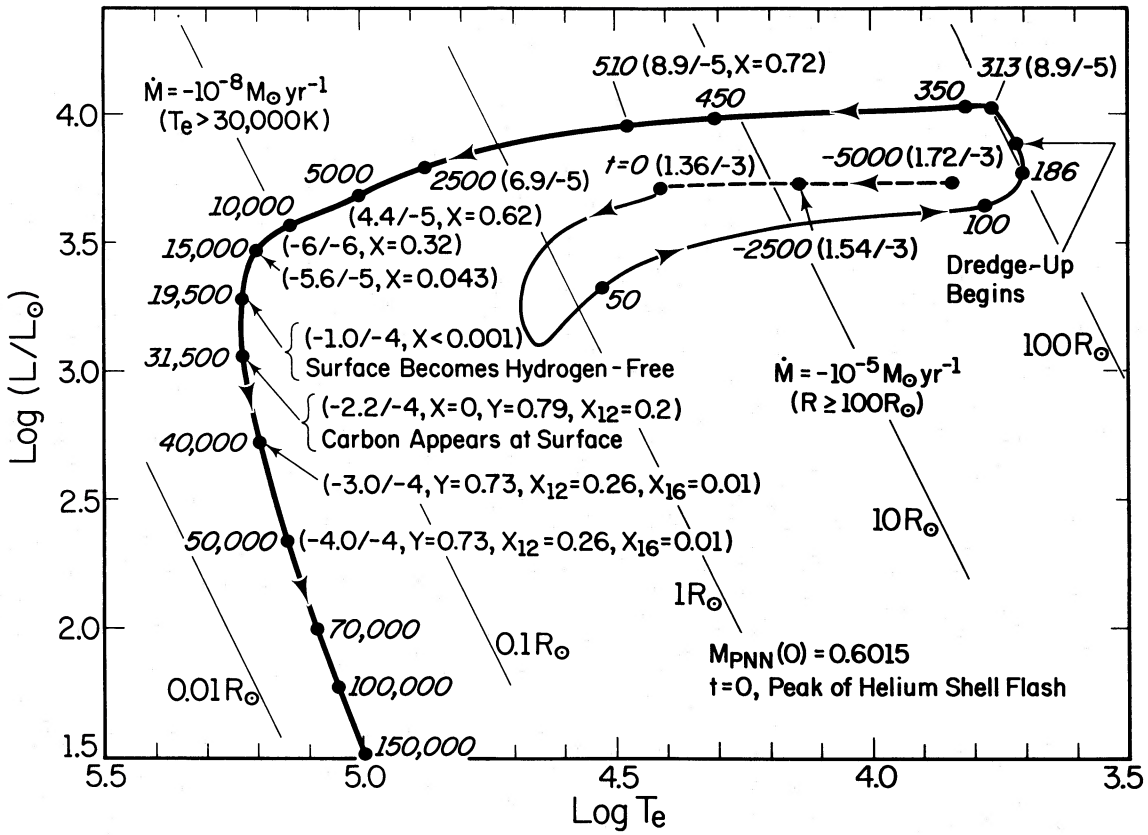

FIG. 11.—Same as Fig. 10 except that the superwind mass loss rate is $\dot{M} = -10^{-5}\ M_\odot\ \mathrm{yr}^{-1}$ when $R > 100\ R_\odot$

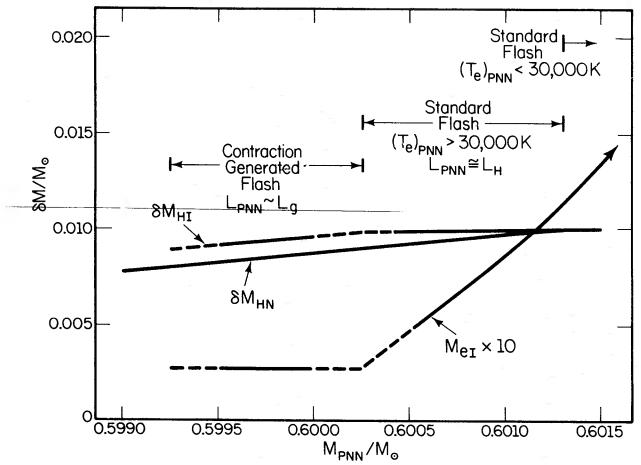

FIG. 12.—Characteristics of models that are relevant for the estimation of the formation frequency of three different types of PNNi: δM_{HN} = mass at the center of the hydrogen profile when the PNN achieves $T_e = 30{,}000$ K, relative to the mass at profile center when the last helium shell flash occurred on the AGB; δM_{HI} = mass at profile center when the final helium shell flash occurs, minus the mass at profile center when the preceding flash occurs. Further, M_{eI} = total stellar mass minus mass at profile center when last flash occurs. For models with stellar mass M_{PNN} in the range 0.5995 $M_\odot$ to 0.6000 $M_\odot$ (or with $\delta M_{HN} = 0.0082$ $M_\odot$ to 0.0087 $M_\odot$), the last helium shell flash occurs after hydrogen burning has ceased (type II models). For models with $M = 0.6005$ $M_\odot$ to 0.6013 $M_\odot$ ($\delta M_{HN} = 0.0092$ $M_\odot$ to 0.0100 $M_\odot$), models experience a helium shell flash when $T_e \geq 30{,}000$ K while hydrogen burning still provides most of the stellar luminosity (type III models). From the nature of the curve for δM_{HI}, it is reasonable to interpolate the actual division between type II and III models to be at about $M_{PNN} \sim 0.6003$ $M_\odot$ ($\delta M_{HN} \sim 0.0090$ $M_\odot$). The division between type I and II is not clear cut, and we shall choose it arbitrarily to be at $M_{PNN} \sim 0.5993$ $M_\odot$ ($\delta M_{HN} \sim 0.0080$ $M_\odot$).

of Table 2 ("guess 1"). These entries are appropriate whether or not a superwind operates, as long as the wind strength ($\dot{M}$) remains constant, independent of phase.

As another example, let us suppose that mass loss on the AGB occurs at three different rates which are related to the mean luminosity during the three major phases: the quiescent hydrogen-burning phase $\dot{M} = \dot{M}_1$, $\tau_1 \sim 0.9\tau_{ip}$, the high-luminosity phase following a helium shell flash $\dot{M} = \dot{M}_2$, $\tau_2 \sim 0.01\tau_{ip}$, and the low-luminosity quiescent helium burning phase $\dot{M} = \dot{M}_3$, $\tau_3 \sim 0.09\tau_{ip}$. If, for $\dot{M}_1$, we adopt equation (5) with $\eta = \frac{1}{3}$ and $M \sim M_H \sim 0.6$ $M_\odot$, we have that $\Delta M_1 \sim 3\Delta M_H$ is the amount of mass lost from the star during the hydrogen-burning phase between pulses. Arbitrarily choosing $\dot{M}_2 \sim 10\dot{M}_1$ and $\dot{M}_3 \sim 0.1\dot{M}_1$, we have that $\Delta M_2 \sim 0.01(\dot{M}_2/\dot{M}_1)3\Delta M_H \sim 0.3\Delta M_H$ and $\Delta M_3 \sim 0.1(\dot{M}_3/\dot{M}_1)3\Delta M_H \sim 0.03\Delta M_H$. Assuming that the probability for departure from the AGB is simply proportional to the amount of mass lost in each phase, we obtain the set of probabilities in row 2 of Table 2 ("guess 2").

As a final example, we again assume that mass loss occurs at three different rates for the hydrogen-burning, high-luminosity helium-burning, and low-luminosity helium-burning phases, but set $\dot{M}_2 \sim 100$ $\dot{M}_1$ and $\dot{M}_3 \sim 0.1\dot{M}_1$. The probabilities in the third row of Table 2 result ("guess 3").

What do the probabilities in Table 2 imply for the frequency of PNNi of mass $M_{PNN} \sim 0.6$ $M_\odot$ which are powered by

TABLE 2

PROBABILITIES OF DEPARTURE FROM THE AGB FOR MODELS OF SIX TYPES

Guess	P_I	P_{II}	P_{III}	P_{IV}	P_V	P_{VI}
1	0.69	0.09	0.09	0.03	0.01	0.09
2	0.69	0.09	0.09	0.03	0.09	0.01
3	0.38	0.05	0.05	0.017	0.50	0.003

helium burning relative to the frequency of those which are powered by hydrogen burning and what do they imply for the fraction of white dwarfs which are non-DA? All models of type I and II burn hydrogen at high temperatures ($T_e \geq 30{,}000$ K) for $\sim$16,000 yr and the average lifetime of models of type III as hot hydrogen burners is, say, 8000 yr. Assuming that the wind which is reactivated during the high-luminosity born-again AGB phase following a helium shell flash reduces envelope mass down to something comparable to or less than 0.0003 $M_\odot$, models of types III–V will not experience a second hydrogen-burning phase. However, models of type VI may depart from the AGB with significantly larger values of M_e than those which depart from the AGB while burning hydrogen (see Fig. 6). Thus such models will experience a second hydrogen-burning phase that lasts much longer at high luminosity than 16,000 yr. Let us suppose that the typical lifetime is $\sim$32,000 yr. Models of types III–V will burn helium at high luminosity for, say, 40,000 yr, while those of type VI will, on average, only spend half of their quiescent helium-burning phase far from the AGB, and we estimate for them a lifetime of $\sim$10,000 yr (they are at higher average luminosity than are other types). Setting $\eta_H \propto 16{,}000(P_I + P_{II} + 0.5P_{III} + 2P_{VI})$ and setting $\eta_{He} \propto 40{,}000(P_{II} + P_{III} + P_{IV} + P_V + 0.25P_{VI})$, we estimate from Table 2 the percentage of all high-luminosity PNNi that are in the helium-burning phase to be $100\eta_{He}/(\eta_H + \eta_{He}) \sim 0.38$ (guess 1), 0.47 (guess 2), and 0.77 (guess 3).

An estimate of DA and non-DA white dwarf frequencies is much more difficult. We estimate, first, that all models of types I and VI will never lose all of their surface hydrogen. Both types experience hydrogen burning at high luminosity and high surface temperature. Hydrogen burning becomes negligible when M_e decreases to $\lesssim 0.00027$ $M_\odot$, regardless of whether it is a wind or nuclear burning that produces this M_e. The main hydrogen-burning phase takes place between $\log L \sim 3.7$ and $\log L \sim 2.7$ and only $\sim$1000 yr is required for $\log L$ to drop from 2.7 to $\sim$1.7. Wind loss at rather high rates operating at fairly low luminosities is therefore required if helium-rich layers ($M_e \sim -(0.00009 - 0.00022)$ $M_\odot$) or carbon-rich layers (M_e more negative than 0.00022 $M_\odot$) are to be exposed, and this does not appear likely.

In contrast, models of type II spend over 35,000 yr at luminosities greater than $\log L \sim 2.7$ and winds ejecting mass at rates as modest as $\dot{M} \sim -(10^{-11}$ to $10^{-9})$ $M_\odot$ yr^{-1} will expose helium- and carbon-rich layers. Since mass loss rates on the order of -10^{-8} $M_\odot$ yr^{-1} are more likely, we therefore expect type II models to become non-DA white dwarfs at high luminosity and high surface temperature.

If we suppose that during the high-luminosity, low surface temperature phase after a helium shell flash, models of types III–V lose mass until $M_e \lesssim$ few $\times 10^{-4}$ $M_\odot$, then mass loss

via a hot wind at a rate $\dot{M} \sim -10^{-8}\ M_\odot\ \mathrm{yr}^{-1}$ will begin to expose helium-rich layers toward the end of the high-luminosity, high surface temperature portion of the helium-burning phase which lasts roughly 40,000 yr.

Adopting this picture, we may predict the number of non-DA (DB for short) white dwarf progenitors relative to the total number of white dwarf progenitors in the luminosity interval $\log L \sim 2.7$–3.7. Defining $n_{\mathrm{DA}} = 16{,}000(P_{\mathrm{I}} + P_{\mathrm{II}} + 0.5P_{\mathrm{III}} + 2P_{\mathrm{VI}}) + 40{,}000(P_{\mathrm{III}} + P_{\mathrm{IV}} + P_{\mathrm{V}} + 0.25P_{\mathrm{VI}})$ and $n_{\mathrm{DB}} = 40{,}000P_{\mathrm{II}}$, we have $n_{\mathrm{DB}}/(n_{\mathrm{DB}} + n_{\mathrm{DA}}) \approx 0.14$ in both guesses 1 and 2. This is rather close to the fraction found in the Green survey (Green and Liebert 1983). For guess 3 we have $n_{\mathrm{DB}}/(n_{\mathrm{DB}} + n_{\mathrm{DA}}) \sim 0.07$ and conclude that perhaps a superwind cannot be confined to the immediate aftermath of a helium shell flash and be two orders of magnitude stronger than the ordinary wind for the same stars.

Models of type I traverse the range $\log L \approx 2.7$–1.7 in only a few thousand years, whereas those of all other types require roughly 60,000 yr. Further mass loss (perhaps now at $\dot{M} \sim -10^{-9}\ M_\odot\ \mathrm{yr}^{-1}$ or less) during this extended phase might be expected to complete the conversion of models of types III–V to non-DA white dwarfs. Beyond $\log L \sim 1.7$, all types cool at about the same rate. Thus for the lowest luminosity white dwarfs we might expect $n_{\mathrm{DA}} \propto P_{\mathrm{I}} + P_{\mathrm{VI}}$, $n_{\mathrm{DB}} \propto P_{\mathrm{II}} + P_{\mathrm{III}} + P_{\mathrm{IV}} + P_{\mathrm{V}}$, or $n_{\mathrm{DB}}/(n_{\mathrm{DA}} + n_{\mathrm{DB}}) \approx 0.22$ (guess 1), 0.30 (guess 2), and 0.62 (guess 3). The first two numbers compare quite favorably with the value $n_{\mathrm{DB}}/(n_{\mathrm{DA}} + n_{\mathrm{DB}}) \sim 0.25$ quoted by Sion (1979).

In summary, the wind-exposure hypothesis accounts quite naturally for the transformation of the surface composition of a fair fraction of white dwarfs during the cooling phase. Because rates of mass loss via a high velocity wind might be expected to be strong functions of both L and T_e, and hence of white dwarf and white dwarf progenitors' mass, and since the amounts of matter which need to be stripped off to expose more highly processed layers are strong functions of progenitor mass, one does not expect each successive transformation to a composition reflective of a greater degree of thermonuclear processing to take place at unique values of T_e or/and L. This last feature of the wind-exposure hypothesis contrasts strongly with the heretofore most widely examined hypothesis for the observed transformations, namely, convective dilution (Strittmatter and Wickramasingh 1971; Baglin and Vauclair 1973; D'Antona and Mazzitelli 1974, 1975, 1979; Koester 1976). The basic idea of the dilution hypothesis is that, when convection first breaks out at and below the surface of a white dwarf, the (hopefully) thin layer of hydrogen will be convected downward into initially pure helium and diluted to values below the limit of detectability.

Unfortunately, the maximum mass that can be contained in a convective layer appears to be incredibly small relative to the initial masses of surface hydrogen expected from evolutionary stellar model calculations. As described by D'Antona and Mazzitelli (1979), the mass in a hydrogen convective shell increases from $\sim 5 \times 10^{-17}\ M_\odot$ to a maximum of $\sim 5 \times 10^{-6}\ M_\odot$ as T_e drops from $\sim$20,000 K to $\sim$13,000 K; the mass in a helium convective shell increases from a $\sim 5 \times 10^{-18}\ M_\odot$ to a maximum of $\sim 5 \times 10^{-6}\ M_\odot$ as T_e drops from $\sim$13,000 K to $\sim$5000 K. In order, then, for the surface hydrogen-to-helium ratio to drop to values consistent with limits provided by spectroscopic analysis of non-DA white dwarfs, say, H/He $< 10^{-4}$, it would be necessary for the mass of the surface layer of hydrogen-rich matter to be less than $\sim 10^{-9}\ M_\odot$ prior to convective dilution. This is much, much smaller than the thickness of the hydrogen profile in an AGB star or in a PNN of any mass (see Fig. 9 for an example when $M_{\mathrm{PN}} \sim 0.6\ M_\odot$).

Is there any process that could reduce the mass of the hydrogen-rich layer to less than $10^{-9}\ M_\odot$ in approximately 40% of all cases and stop far short of this in the other 60%? It has recently been suggested (Fontaine and Michaud 1984) that chemical diffusion may carry hydrogen inward from the base of the hydrogen profile to such high temperatures that it can be burned thermonuclearly. That hydrogen can continue to burn as a white dwarf cools, even in the absence of chemical diffusion, has been demonstrated by Iben and Tutukov (1984*b*) who show that burning by the *p-p* chains continues at a significant rate at the base of a hydrogen-rich surface layer until white dwarf luminosity drops below $\sim 10^{-4}\ L_\odot$ and that, for luminosity in the range $10^{-3} \lesssim L/L_\odot \lesssim 2 \times 10^{-2}$, the bulk of the surface luminosity is actually provided by the energy released in hydrogen burning. However, over the entire lifetime of the cooling white dwarf (assumed to be of constant mass = $0.6\ M_\odot$), the mass of the hydrogen-rich surface layer is reduced only by $\sim 10^{-4}\ M_\odot$, from $2.7 \times 10^{-4}\ M_\odot$ to $1.5 \times 10^{-4}\ M_\odot$. Whether or not chemical diffusion can offset the tendency for hydrogen to be buoyed upward by the effects of gravitational diffusion and whether the burning induced by inward diffusion is much more dramatic (by five orders of magnitude) than that which occurs in the absence of chemical diffusion has yet to be determined. In any case, there is no obvious natural way to explain the statistics of DA versus non-DA white dwarfs solely in terms of a burning away of the hydrogen at the base of the envelope unless the burning process is either preceded by or abetted by a wind mass loss that can by itself significantly reduce the envelope mass in an easily identified 40% of all cases. It therefore follows that, even if it is not a differential wind *exposure* that is totally responsible for the production of non-DA white dwarfs, some variant such as differential wind *reduction* (prior to or concomitant with some other reduction mechanism such as inward diffusion and burning) is essential for producing non-DA's.

VIII. COMMENTS ON THE RELEVANCE OF QUASI-STATIC PNN MODELS FOR UNDERSTANDING THE NEBULAE A30 AND A78, R CORONAE BOREALIS STARS, AND FG SAGITTAE

Models of the sort described in this paper have been variously discussed in connection with several rare but fascinating objects. In particular, the hydrogen-poor knots ejected by the central stars in the nebulae A30 and A78 (Hazard *et al.* 1980; Jacoby and Ford 1983) have been associated with PNN models of type II (Iben *et al.* 1983); the peculiar abundances in R Coronae Borealis stars (Searle 1961; Danziger 1965; Orlov and Rodrigues 1974; Schönberner 1975; Cottrell and Lambert 1982; Hunger, Schönberner, and Steenbock 1982) have been attributed to exposure of highly processed matter following a helium shell flash in PNNi of types II–IV (Renzini 1979); and the rapid ($dT_e/dt \sim -250$ K yr^{-1}) expansion of the PNN FG Sagittae (Herbig and Boyarchuck 1968; Archipova *et al.* 1978; Stone 1979) and

the accompanying apparent change in surface composition (Langer, Kraft, and Anderson 1974; Kipper and Kipper 1977; Kipper 1978) have been cited as proof that FG Sagittae has experienced a helium shell flash (Paczyński 1970; Schönberner 1979) and has, by some means, brought to the surface some of the matter freshly processed in the burning shell (Langer, Kraft, and Anderson 1974; Christy-Sackmann and Despain 1974; Schönberner 1979, 1983; Sackmann 1980).

Although the interpretation of these objects is terms of events triggered by a helium shell flash in a PNN is qualitatively quite attractive, several quantitative difficulties with the interpretation remain. In the cases of A30 and A78, the main difficulty is that the low velocities of the knots, if interpreted in the usual fashion, are not consistent with the expected radius of the PNN when hydrogen-free layers are exposed. The knots have velocities of 22–25 km s^{-1} (Reay, Atherton, and Taylor 1983), which are similar to velocities of matter in winds ejected from cool giants and to velocities of PN material which has presumably been ejected from a precursor AGB star of large radius. They are quite small compared with the typical velocities (1000–3000 km s^{-1}) of matter flowing from hot, compact PNNi. The obvious inference is that helium-rich layers are ejected when the PNN becomes a born-again AGB star of large radius. Disconcertingly, the quasi-static calculations suggest that, for type II models, the maximum radius attainable following a helium shell flash is directly proportional to the mass left in the hydrogen-rich zone at the outer edge of the star (see Fig. 2); any reduction in the mass of the hydrogen-rich "skin" due to wind ejection will force the radius of the PNN to drop and, by the time hydrogen-free material is exposed, the PNN is no longer of giant dimensions. This is true also for model PNNi of types III and IV. One may resolve this discrepancy by supposing that (1) the quasi-static approximation is a singularly poor one and, in the real case, additional sources of pressure due to macroscopic motions generated by the flash maintain the star at giant dimensions, even after its hydrogen-rich skin is removed; or (2) the hydrogen skin is converted into a helium skin by burning in the course of the flash while the PNN is still compact and is then ejected at low velocity by a mechanism totally different from that which produces a wind in compact PNNi.

A further difficulty in understanding A30 and A78 in terms of models of type II is that the postflash hydrogen profile in type II models is a step function, with matter below the hydrogen-rich skin containing no ^{14}N, an element which is prominently featured in the spectrum of the central star of A30 (Greenstein 1981; Heap 1982). This discrepancy between actual and expected composition might be taken as evidence that, in a real PNN of type II, hydrogen is rekindled and completely converted into ^4He (^{14}N is not burned in this situation) in a convective zone which is detached from the convective zone in which helium-burning reactions (including the destruction of ^{14}N) take place during the peak of the helium shell flash. It could also be explained by supposing that the progenitor of A30 is representative of PNN models of type III or of type IV. In these models, a relatively thick layer which contains only products of complete hydrogen burning via the CNO cycle (mostly ^4He, with the abundance of ^{14}N much greater than the abundance of either ^{16}O or ^{12}C) separates the hydrogen-rich skin from the layers which have experienced helium at burning (and destruction of ^{14}N). However, also in this case, the problem of accounting for knot velocities remains.

The difficulty with the interpretation of R CrB stars as PNNi which have experienced a helium shell flash and then lost all of their surface hydrogen is essentially the same as the difficulty in understanding A30 and A78: how can a PNN achieve a large radius ($L \sim$ few $\times 10^3$ $L_\odot - 10^4$ $L_\odot$, $\log T_e \sim 3.8$) and at the same time have no hydrogen at its surface? The difficulty is much more serious than in the A30 and A78 cases since the concern about large radii does not hinge on indirect inference—the stars with hydrogen-free surfaces are *now* observed to be quite blatantly large.

The R CrB stars are known to pulsate and to lose mass in "puffs" (e.g., Herbig 1949; Feast 1979). Could it be, once again, that macroscopic motions generated by the flash provide sufficient additional pressure to maintain these stars at large radii? Or does the high opacity of carbon at low temperatures (perhaps considerably underestimated in the models) take the place of a high hydrogen-related opacity in maintaining them at large radii (Iben and Renzini 1983)? Another possibility is that R CrB stars are not single PNN stars at all, but are instead products of the evolution of appropriately exotic binary evolution (see, e.g., Iben and Tutukov 1984*a*; Webbink 1984).

The final conundrum is posed by FG Sagittae, which has frequently been eulogized as the epitome of stars which, following a final helium shell flash, bring to the surface products of exotic neutron-capture nucleosynthesis that has been imagined to take place during this final flash. The most compelling circumstantial evidence that FG Sagittae may be a bona fide example of a PNN of type III which has experienced a flash in the recent past is the fact that, over the past few decades, it has exhibited an extremely rapid growth in radius at nearly constant luminosity. It is clear that the rate at which FG Sge is currently evolving to the red in the H-R diagram [$dT_e/dt \sim -(200\text{–}250)$ K yr^{-1}] is not inconsistent with the rate at which theoretical models of type III or IV evolve to the red after a flash (see, e.g., the evolution from $t = 0$ to $t = 100$ yr in Figs. 10 and 11).

It is worth commenting that the FG Sge phenomenon may also be direct evidence that the ejection of a nebular shell is not always, if indeed usually, correlated with a helium shell flash. For, as we have seen in previous sections, type III PN evolution can occur only if the progenitor of the PN is well into the interpulse phase ($0.88 \gtrsim \delta M_H/\Delta M_H \gtrsim 0.97$) *before* it departs from the AGB as a consequence of PN ejection.

The expansion age of the primary planetary nebular shell surrounding FG Sge may be used to place limits on the core mass of the central star. Estimating the distance to the nebula as 2500 pc, Flannery and Herbig (1973) estimate this expansion age to be approximately 6000 yr. If this age were to be identified with the time elapsing between two successive thermal pulses on the AGB (Langer, Kraft, and Anderson 1974; Christy-Sackmann and Despain 1974; Fadeyev and Tutukov 1978), one would estimate, using $\tau_{ip} \sim 2.5 \times 10^5$ $(0.6\ M_\odot/M_H)^{10}$ yr, that $M_H \sim 0.87\ M_\odot$. Or, supposing the distance to FG Sge to be more like 2500 pc $\times$ 1.5, so that the expansion age is closer to 9000 yr, one would estimate $M_H \sim 0.84\ M_\odot$. However, we have seen that type III PN evolution requires the first departure from the AGB to occur

"long" after the last flash on the AGB; the identification of τ_{ip} with τ_{ex} is therefore clearly inappropriate. Assuming, more reasonably, that the fading time given by equation (9) is at least as large as τ_{ex}, and again choosing $\tau_{ex} \sim 6000$ yr, we have that $M_H \gtrsim 0.66\ M_\odot$. In general, we may write

$$M > M_1 = 0.66(2500\text{ pc}/D)^{1/10}\ , \qquad (11)$$

where D is the distance to FG Sge in parsecs.

The "expansion age" is inversely proportional to the *current* velocity of expansion, and there is some indication that expansion velocity increases with time. For example, Kaler (1983) finds that typical expansion velocities of "small" PNe (a type to which FG Sge belongs) are 10–15 km s^{-1}, whereas expansion velocities of large nebulae range from 10–40 km s^{-1}. It is not out of the question that the actual expansion age of FG Sge for $D = 2500$ pc is as large as 12,000 yr. If this were the case, then the coefficient 0.66 in equation (11) becomes 0.62.

An additional way to estimate the mass of FG Sge is to insert a distance-dependent estimate of FG Sge's bolometric luminosity into the core mass–luminosity relationship given in equation (2). Using the bolometric correction chosen by Fadeyev and Tutukov (1978), we have

$$M \sim M_2 = 0.5 + 0.096(D/2500\text{ pc})^2\ . \qquad (12)$$

Both equations (11) and (12) are satisfied if $D \sim 3100$ pc and $M \sim 0.645$.

Yet another way (Fernie 1975) to estimate the mass of the central star is to make use of the results of pulsation theory (and of one additional theoretical constraint) in conjunction with the observed color and pulsation characteristics of FG Sge (Papousek 1972; Archipova 1973; Archipova *et al.* 1980). This has been done by Whitney (1978) to estimate $M \sim 0.4\ M_\odot$ and by Fadeyev and Tutukov (1981) to estimate $M \sim 0.8\ M_\odot$. The lower of these two estimates may be ruled out since the minimum core mass for thermal pulses to occur is $\sim 0.53\ M_\odot$, and the higher one gives a PNN evolutionary time too short compared with the PN expansion age. A reexamination of the implications of the pulsation characteristics of FG Sge is therefore in order.

From linear pulsation theory one may obtain a relationship between pulsation period, stellar radius, and mass (e.g., as abstracted by Böhm-Vitense *et al.* 1974 from calculations of Tuggle and Iben 1972):

$$P_F = QR^{3/2}/M^{1/2} \approx 0.0232(R/M)^{0.22}R^{3/2}/M^{1/2}\ . \qquad (13)$$

Here P_F is the period (in days) of the fundamental radial mode, and M and R are in solar units. Making use of equation (2), which relates L and M ($\sim M_H$), and of the definition $L/R^2 = (T_e/T_{e\odot})^4$, where $T_{e\odot}$ is the Sun's effective temperature, we have finally that

$$M \sim M_3 = 0.5 + 0.0010M^{0.84}{P_F}^{1.16}(T_e/T_{e\odot})^4\ . \qquad (14)$$

Setting $M \sim 0.64$ on the right-hand side of equation (14) we have

$$M_3 \sim 0.5 + 0.069(P_F/90\text{ d})^{1.16}(T_e/5000\text{ K})^4\ . \qquad (14')$$

If we adopt $P_F \sim 90$ days and $T_e \sim 5000$ K (as given in 1979 by Archipova informally to Fadeyev and Tutukov 1981), equation (14′) gives $M \sim 0.57$. This is considerably less than the estimate of 0.645 which follows from equations (11) and (12). The only way to reconcile the two estimates is to suppose that the surface temperature of FG Sge, when $P \sim 90$ days, is in excess of 6000 K. Can it be that mass loss from the surface (Langer, Kraft, and Anderson 1974 entertain rates as large as $10^{-6}\ M_\odot\ \text{yr}^{-1}$) creates an atmosphere which partially hides the "real," hotter photosphere (the one which would obtain in the absence of mass loss)?

Although the time scale for expansion is quite comparable to that of postflash PNN models, the evidence most frequently cited in recent years as proof that FG Sge has experienced a flash is that the abundances of neutron-rich isotopes at the stellar surface appeared to increase over the period 1965–1972 (Langer, Kraft, and Anderson 1974; Kipper 1976). The standard interpretation of this apparent increase is that neutron-rich isotopes were produced in the helium-burning convective shell during the flash which forced FG Sge to expand and were then brought to the surface during the expansion phase.

Unfortunately, there are several features of the estimated abundances and of the apparent abundance changes that are difficult to reconcile with the nucleosynthesis characteristics of theoretical models of helium flashing stars of core mass relevant to FG Sge. Furthermore, appropriate models which do dredge up fresh products of shell nucleosynthesis do so during a phase which *follows* that which FG Sge has presumably been passing through over the past few decades.

The remarkable features of the estimated abundances and their apparent changes are: (1) the neutron-rich isotopes appear to be made by the so-called slow neutron capture process and are in the solar system distribution; (2) the abundances of the *s*-process isotopes relative to one another do not appear to change as their absolute values increase; and (3) the abundance of carbon appears to *decrease* at the same time that the *s*-process isotopes appear to *increase* in abundance.

The first feature is a bit surprising since the only source of neutrons (the ^{22}Ne source) which has been demonstrated to produce *s*-process isotopes in the solar system distribution in a natural way (Iben 1975*b*; Truran and Iben 1977) does not operate effectively in stars of core mass less than ~ 0.9–$1.0\ M_\odot$ (Becker 1981; Iben 1982), whereas the ^{13}C neutron source, which may operate in stars of the relevant core mass is expected to produce neutron-rich isotopes in a non–solar-system–like distribution (Iben and Renzini 1982).

The second feature is surprising since a model star of the relevant core mass will not have experienced a sufficient number of prior helium shell flashes to establish an asymptotically stable distribution of neutron-rich isotopes (Truran and Iben 1977). That is, the distribution of isotopes emerging after each flash is expected to be different from that emerging from previous flashes, and to be considerably different from the distribution of such isotopes in the envelope prior to dredge-up.

The third feature is the most puzzling of all. The abundance per gram of ^{12}C that is formed in the convective shell during a thermal pulse is approximately 100 times larger than solar. Since ^{12}C and the neutron-rich isotopes are formed simultaneously in the same convective region, if these latter isotopes are brought to the surface, then fresh ^{12}C must also be brought to the surface. Even if the models have

totally missed the mark with respect to describing details of the production of *s*-process isotopes, it is exceedingly difficult to imagine a mechanism which can selectively bring heavy elements to the surface in the ratio in which they are formed while at the same time leaving behind a much lighter element.

The final, and perhaps most perplexing, feature of the alleged dredge-up episode in FG Sge is that it occurs before theoretical models suggest that it should. In luminous post-flash models which have surface temperatures as large as those exhibited by FG Sge during the period of apparent surface abundance changes, convection is confined to a very thin layer near the surface. Envelope convection does not extend downward even as far as the outer edge of the hydrogen profile until the model becomes a born-again AGB star at a luminosity larger than that characteristic of the preflash stage (at the positions noted in Figs. 10 and 11). This is a result that is independent of core mass, at least for $M \gtrsim 2\ M_\odot$ (Wood 1983). Further, dredge-up of material that was earlier in a helium-burning convective shell does not occur in a star of Population I composition unless $M_H \gtrsim 0.65\ M_\odot$ (Iben 1983; Wood 1983), and it does not do so even then until the model has progressed much further upward along the AGB than has FG Sge.

The heretical conclusion to which one appears to be forced is that FG Sge has *not* just completed dredging up freshly produced *s*-process isotopes. If this is so, then the fault must lie in the estimates of surface abundances. We have already remarked that, in order to reconcile a pulsation-related mass with the limiting mass suggested by the expansion age of the nebula, (1) an effective temperature considerably larger than that indicated by the colors is required, and (2) the presence of a strong wind might be responsible for the formation of a nonstandard atmosphere that accounts for this effect. Could the same explanation account for the apparent abundance changes which are so difficult to understand in terms of theoretical models of PNNi?

It is with considerable pleasure that I thank Alvio Renzini for introducing me to the mysteries and delights of the planetary nebula formation problem and for stimulating me to engage in hopefully relevant model explorations. It is with equal pleasure that I thank Aleksandr V. Tutukov for forcing me to examine the ultimate consequences of every idle speculation and to prepare a logical (and hopefully sometimes reasonable) justification for each one. James Kaler and Alvio Renzini's careful reading of the manuscript and their suggestions for improving the presentation are very much appreciated, and conversations with James Liebert concerning the effect of mass loss versus the effect of mixing on changing surface composition were enlightening. Useful conversations with Jules Cahn, James MacDonald, Georges Michaud, James Truran, Detlef Schönberner, Ronald Webbink, and Volker Weidemann are additionally acknowledged.

Thanks finally to the University of Illinois Research Board for providing funds for the extensive computer calculations required for this investigation, to George Badger and Michael Randal for facilitating the computations, and to Deana Griffin for her typically superb translations of illegible drafts.

REFERENCES

Archipova, V. P. 1973, *Mem. Soc. Roy. Sci. Liège*, 6 Sèr., **5**, 477.
Archipova, V. P., Zaitseva, G. V., Noskova, R. I., and Saveljeva, M. V. 1980, *Astr. Tsirk.*, No. 1111, p. 1.
Baglin, A., and Vauclair, G. 1973, *Astr. Ap.*, **27**, 307.
Baud, B., and Habing, H. J. 1983, in *Planetary Nebulae*, ed. R. D. Flower (Dordrecht: Reidel), p. 530.
Baud, B., Habing, H. J., Mathews, H. E., and Winnberg, A. 1981, *Astr. Ap.*, **95**, 156.
Becker, S. A. 1981, in *Physical Processes in Red Giants*, ed. I. Iben, Jr. and A. Renzini (Dordrecht: Reidel), p. 141.
Böhm-Vitense, E., Szkody, P., Wallerstein, G., and Iben, I., Jr. 1974, *Ap. J.*, **194**, 125.
Castor, J. I., Lutz, J. H., and Seaton, M. J. 1981, *M.N.R.A.S.*, **194**, 547.
Christy-Sackmann, I.-J., and Despain, K. 1974, *Ap. J.*, **189**, 523.
Cottrell, P. L., and Lambert, D. L. 1982, *Ap. J.*, **261**, 595.
D'Antona, F., and Mazzitelli, I. 1974, *Ap. Space Sci.*, **27**, 137.
———. 1975, *Astr. Ap.*, **44**, 253.
———. 1979, *Astr. Ap.*, **74**, 161.
Danziger, I. J. 1965, *M.N.R.A.S.*, **130**, 199.
de Jong, T. 1983, *Ap. J.*, **274**, 252.
Fadeyev, Yu. A. 1982, *Ap. Space Sci.*, **86**, 143.
Fadeyev, Yu. A., and Tutukov, A. V. 1981, *M.N.R.A.S.*, **195**, 811.
Feast, M. W. 1975, in *IAU Symposium 75, Variable Stars and Stellar Evolution*, ed. V. G. Sherwood and L. Plant (Dordrecht: Reidel), p. 129.
Fernie, J. D. 1975, *Ap. J.*, **200**, 392.
Flannery, B., and Herbig, G. H. 1973, *Ap. J.*, **183**, 491.
Fontaine, G., and Michaud, G. 1984, *Ap. J.*, in press.
Fontaine, G., and Van Horn, H. M. 1976, *Ap. J. Suppl.*, **31**, 467.
Frogel, J. A. 1983, in preparation.
Frogel, J. A., and Iben, I., Jr. 1983, in preparation.
Fujimoto, M. Y. 1977, *Pub. Astr. Soc. Japan*, **29**, 331.
Fusi-Pecci, F., and Renzini, A. 1976, *Astr. Ap.*, **46**, 447.
Gingold, R. 1974, *Ap. J.*, **193**, 177.
———. 1976, *Ap. J.*, **204**, 116.
Green, R., and Liebert, J. 1983, private communication.
Greenstein, J. 1981, *Ap. J.*, **245**, 124.
Härm, R., and Schwarzschild, M. 1975, *Ap. J.*, **200**, 324.
Hazard, C., Terlevich, B., Morton, D. C., Sargent, W. L. W., and Ferland, G. 1980, *Nature*, **285**, 463.
Heap, S. R. 1979, in *IAU Symposium 83, Mass Loss and Evolution of O-Type Stars*, ed. P. S. Conti and C. W. H. de Loore (Dordrecht: Reidel), p. 99.
———. 1980, *Bull. AAS*, **12**, 540.
———. 1982, in *IAU Symposium 99, Wolf-Rayet Stars: Observations, Physics, and Evolution*, ed. C. W. H. de Loore and A. Willis (Dordrecht: Reidel), p. 423.
———. 1983, in *IAU Symposium 103, Planetary Nebulae*, ed. R. D. Flower (Dordrecht: Reidel), p. 375.
Herbig, G. H. 1949, *Ap. J.*, **110**, 143.
Herbig, G. H., and Boyarchuk, A. A. 1968, *Ap. J.*, **153**, 397.
Hunger, K., Schönberner, D., and Steenbock, W. 1982, *Astr. Ap.*, **107**, 93.
Iben, I., Jr. 1975*a*, *Ap. J.*, **196**, 525.
———. 1975*b*, *Ap. J.*, **196**, 549.
———. 1977, *Ap. J.*, **217**, 788.
———. 1982, *Ap. J.*, **260**, 821.
———. 1983, in preparation.
Iben, I., Jr., Kaler, J. B., Truran, J. W., and Renzini, A. 1983, *Ap. J.*, **264**, 605.
Iben, I., Jr., and Renzini, A. 1982, *Ap. J. (Letters)*, **263**, L23.
———. 1983, *Ann. Rev. Astr. Ap.*, **21**, 271.
Iben, I., Jr., and Tutukov, A. V. 1984*a*, *Ap. J. Suppl.*, in press.
———. 1984*b*, *Ap. J.*, in press.
Jacoby, G. H., and Ford, H. C. 1983, *Ap. J.*, **266**, 298.
Kaler, J. B. 1974, *A.J.*, **79**, 594.
———. 1983, private communication.
Kipper, T. A. 1978, *Soviet Astr. Letters*, **4**(3), 153.
Kipper, T. A., and Kipper, M. A. 1977, *Soviet Astr. Letters*, **3**(5), 220.
Knapp, G. R., Philips, T. G., Leighton, R. B., Lo, K. Y., Wannier, P. G., and Wootten, H. A. 1982, *Ap. J.*, **252**, 616.
Koester, D. 1976, *Astr. Ap.*, **52**, 415.
Koester, D., Schulz, H., and Weidemann, V. 1979, *Astr. Ap.*, **76**, 262.
Kwok, S. 1982, *Ap. J.*, **258**, 280.
———. 1983, in *IAU Symposium 103, Planetary Nebulae*, ed. R. D. Flower (Dordrecht: Reidel), p. 293.
Kwok, S., Purton, G. R., and Fitzgerald, P. M. 1978, *Ap. J. (Letters)*, **219**, L125.
Langer, G. E., Kraft, R. P., and Anderson, K. S. 1974, *Ap. J.*, **189**, 509.
Liebert, J. 1979, in *IAU Colloquium 53, White Dwarfs and Variable Degenerate Stars*, ed. H. M. Van Horn and V. Weidemann (Rochester: University of Rochester), p. 146.

Liebert, J. 1980, *Ann. Rev. Astr. Ap.*, **18**, 363.
Oke, B., Weidemann, V., and Koester, D. 1984, *Ap. J.*, in press.
Orlov, M. Ya., and Rodrigues, M. H. 1974, *Astr. Ap.*, **31**, 203.
Paczyński, B. 1970, *Acta Astr.*, **20**, 47.
Papousek, J. 1972, *Contr. Astr. Inst. University Brno*, **2**, No. 18.
Perinotto, M. 1983, in *IAU Symposium 103, Planetary Nebulae*, ed. R. D. Flower (Dordrecht: Reidel), p. 323.
Perinotto, M., Benvenuti, P., and Cacciari, C. 1981, in *IAU Colloquium 59, Effects of Mass Loss on Stellar Evolution*, ed. C. Chiosi and R. Stalio (Dordrecht: Reidel), p. 45.
Reay, N. K., Atherton, I. D., and Taylor, K. 1983, in *IAU Symposium 103, Planetary Nebulae*, ed. R. D. Flower (Dordrecht: Reidel), p. 508.
Reimers, D. 1975*a*, *Mem. Soc. Roy. Sci. Liège*, 6e Sèr., **8**, 369.
———. 1975*b*, in *Problems in Stellar Atmospheres and Envelopes*, ed. B. Baschek, W. H. Hegel, and G. Traving (Berlin: Springer), p. 229.
Renzini, A. 1979, in *Stars and Star Systems*, ed. B. E. Westerlund (Dordrecht: Reidel), p. 155.
———. 1981*a*, in *Physical Processes in Red Giants*, ed. I. Iben, Jr., and A. Renzini (Dordrecht: Reidel), p. 431.
———. 1981*b*, in *Effects of Mass Loss on Stellar Evolution*, ed. C. Chiosi and R. Stalio (Dordrecht: Reidel), p. 319.
———. 1982, in *IAU Symposium 99, Wolf-Rayet Stars*, ed. C. de Loore and A. J. Willis (Dordrecht: Reidel), p. 413.
———. 1983, in *IAU Symposium 103, Planetary Nebulae*, ed. R. D. Flower (Dordrecht: Reidel), p. 267.
Rose, W. R., and Smith, R. L. 1969, *Ap. J.*, **159**, 903.
Sackmann, I.-J. 1980, *Ap. J. (Letters)*, **241**, L37.
Schönberner, D. 1975, *Astr. Ap.*, **44**, 383.
———. 1979, *Astr. Ap.*, **79**, 108.
———. 1981, *Astr. Ap.*, **103**, 119.
Schönberner, D. 1983, *Ap. J.*, **272**, 708.
Schönberner, D., and Weidemann, V. 1983, in *IAU Symposium 103, Planetary Nebulae*, ed. R. D. Flower (Dordrecht: Reidel), p. 359.
Searle, L. 1961, *Ap. J.*, **133**, 531.
Schatzman, E. 1958, *White Dwarfs* (Amsterdam: North-Holland).
Shklovski, I. S. 1956, *Astr. Zh.*, **33**, 315.
Sion, E. M. 1979, in *IAU Colloquium 53, White Dwarfs and Variable Degenerate Stars*, ed. H. M. Van Horn and V. Weidemann (Rochester: University of Rochester), p. 245.
Sion, E. M., and Liebert, J. 1977, *Ap. J.*, **213**, 468.
Stone, R. P. S. 1979, *Pub. A.S.P.*, **91**, 389.
Strittmatter, P. A., and Wickramasingh, D. T. 1971, *M.N.R.A.S.*, **152**, 47.
Tuchman, Y., Sack, N., and Barkat, Z. 1979, *Ap. J.*, **234**, 217.
Tuggle, R. S., and Iben, I., Jr. 1973, *Ap. J.*, **186**, 593.
Truran, J. W., and Iben, I., Jr. 1977, *Ap. J.*, **150**, 961.
Vauclair, G., and Reisse, C. 1977, *Astr. Ap.*, **61**, 415.
Webbink, R. 1984, *Ap. J.*, **277**, 355.
Weidemann, V. 1975, in *Problems in Stellar Atmospheres and Envelopes*, ed. B. Baschek, W. H. Kegel, and G. Traving (Berlin: Springer), p. 173.
Werner, M. W., Beckwith, S., Gatley, I., Sellgen, K., Berriman, G., and Whiting, D. L. 1980, *Ap. J.*, **239**, 540.
Whitney, C. A. 1978, *Ap. J.*, **220**, 245.
Willson, L. A. 1981, in *Physical Processes in Red Giants*, ed. I. Iben, Jr. and A. Renzini (Dordrecht: Reidel), p. 225.
Wood, P. R. 1974, *Ap. J.*, **190**, 609.
———. 1981, in *Physical Processes in Red Giants*, ed. I. Iben, Jr. and A. Renzini (Dordrecht: Reidel), p. 205.
———. 1983, in preparation.
Wood, P. R., Bessell, M. S., and Fox, M. W. 1983, *Ap. J.*, **272**, 99.
Wood, P. R., and Cahn, J. C. 1977, *Ap. J.*, **211**, 499.

ICKO IBEN, JR.: Department of Astronomy, University of Illinois, 341 Astronomy Building, Urbana, IL 61801-3000